Supporting Information

Primary Amines from Alkenes and Carbonyl Compounds: Highly Selective Ru-Catalyzed Hydrogenation of Oximes

‡Kevin Hares, ‡Hannes W. Wegener, Thomas F. H. Roth, René Reichert, Dieter Vogt, and Thomas Seidensticker*

Author Address

Laboratory of Industrial Chemistry, Department of Biochemical and Chemical Engineering, TU Dortmund University, Emil-Figge-Str. 66, 44227 Dortmund

* Dr. Thomas Seidensticker, Laboratory of Industrial Chemistry, Department of Biochemical and Chemical Engineering, TU Dortmund University, Emil-Figge-Str. 66, 44227 Dortmund.
Phone: +49 231 7552310
Mail: thomas.seidensticker@tu-dortmund.de
Homepage: https://tc.bci.tu-dortmund.de/

‡ These authors contributed equally to this work

Table of Contents

SI 1. Used Chemicals and Materials

All chemicals used within this work are given in Table S 1.

Table S 1: Used chemicals and their purity and supplier.

Name	Purity / %	Brand
1,4-dioxane	99	Merck
1-Octene		TCI
1-Pentene	97	TCI
2,6-Bis(di-t-butylphosphinomethyl)pyridine	99	abcr
2-Ethylbutyraldehyde		TCI
2-Furaldehyde	98	Alfa Aesar
6-bromopicolinaldehyde oxime	99	Synthesized by Hansmann Group at TU Dortmund
Anisol	99	Carl Roth
Benzaldehyde	99.5	Alfa Aesar
Bis(2-diphenylphosphinoethyl)phenylphosphin	97	Abcr
Citronellal	93	Acros Organics
Cyclohexanone oxime	97	Alfa Aesar
DBU	98	Carl Roth
Dppe	98	Thermo Scientific
Hexanal	98	Carl Roth
Hydroxylamine	50	Sigma Aldrich
Methyl 10-Undecenoate	96	TCI
Nonanal	97	Carl Roth
Pentanal	97	Merck
Pivalaldehyde	97	TCI
Potassium hydroxide	85.7	Carl Roth
Potassium tert butoxide	97	Thermo Scientific
$Ru(acac)_3$		TCI
Triphenylphosphine	99	abcr
Triphos	97	Alfa Aesar
Xantphos	98	

SI 2. Preliminary Experiments

Before parameter optimization, experiments were performed to set the limits for optimization. Screening experiments were performed in 20 mL autoclaves equipped with a magnetic stirring bar to get a first impression of the reactions. A ruthenium $Ru(acac)_3$ / dppe system was chosen as a benchmark, and different solvents were tested.

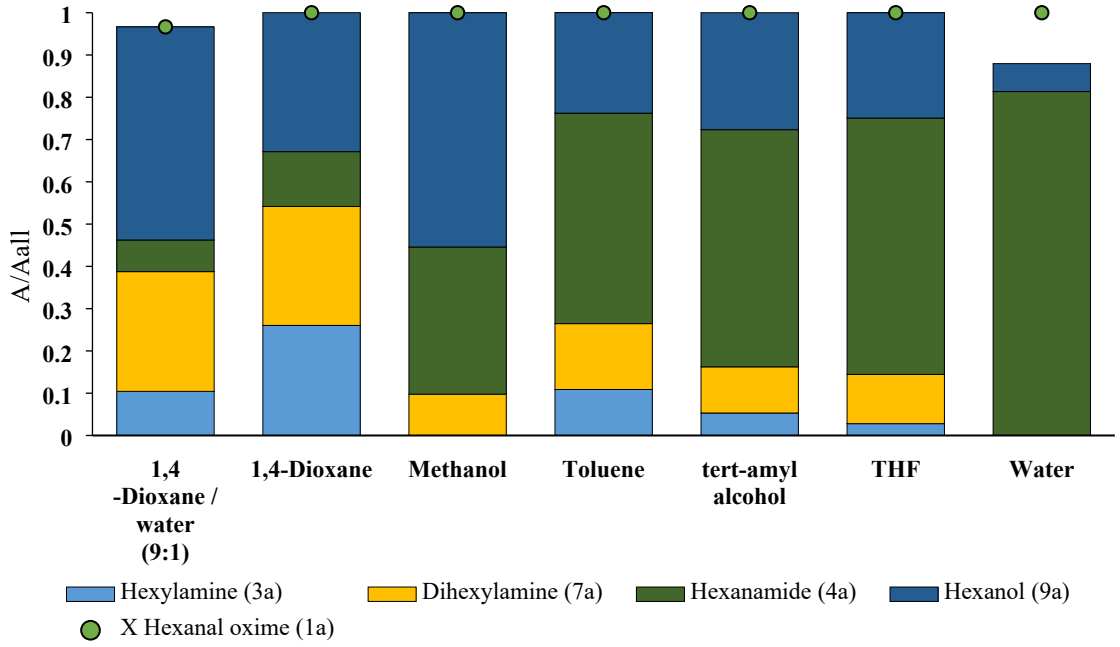

Figure S 1: First solvent screening in 20 ml autoclaves. The ratio of substance area to overall area in GC/FID chromatogram for different solvents (Reaction conditions: Hexanal oxime (**1a**) (1 mmol), $Ru(acac)_3$ (0.01 eq.), dppe (0.02 eq.), K_2CO_3 (0.025 eq.), solvent (2 mL; $p(H_2)$ = 10 bar, 160 °C, 18 h).

The desired amine was detected with all the solvents investigated except for water. The highest amount of hexylamine (**3a**) was found with 1,4-dioxane as solvent. An interesting observation is that the amount of hexanamide (**4a**) seems to increase with the idle time of the prepared reactor. All the reactions presented were carried out in parallel in separate 20 mL autoclaves and charged in the reverse order shown in the graph. The longest time after the preparation of the reactor seems to have the highest amount of amide, i.e., water. A possible explanation is that the active catalyst only forms under reaction conditions and performs the Beckmann rearrangement first. Since dioxane had the best selectivity for the desired primary amine, it was the solvent of choice. To observe the formation of different compounds during the reaction a larger 100 mL reactor was chosen, and samples were taken approximately every hour.

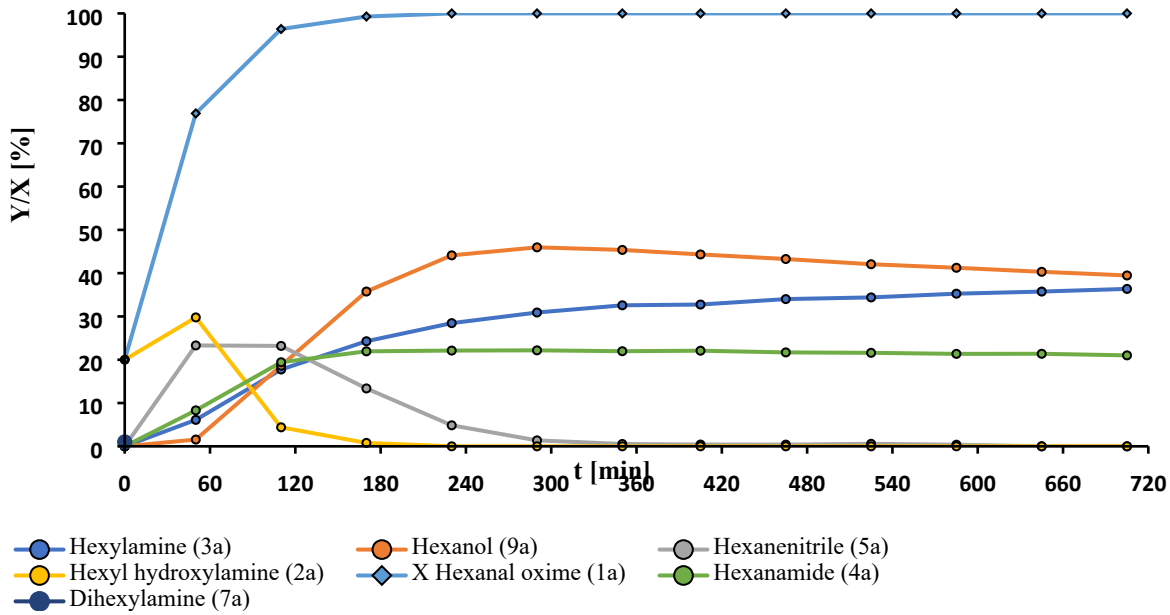

Figure S 2: Reaction profile for ruthenium catalyzed hydrogenation of hexanal oxime (**1a**) with KOH as basic additive and triphos as ligand, reaction E (Reaction conditions: Hexanal oxime (**1a**) (25 mmol), $Ru(acac)_3$ (0.005 eq.), triphos (0.01 eq.), KOH (0.025 eq.), 1,4-dioxane (50 mL), $p(H_2)$ = 10 bar, 160 °C, 12 h).

Amide formation stops after complete conversion of the hexanal oxime (**1a**) and is not consumed afterward. Relatively large amounts of alcohol and nitrile formation were also observed. Interestingly, the alcohol is converted under the present reaction conditions, which the presence of ammonia can explain. The ammonia is formed when the oxime reverts to hydroxylamine and the aldehyde since both are readily hydrogenated under the given conditions. After the reaction, ammonia could be detected with a hand-held ammonia detector.

To avoid the reverse reaction and Beckmann rearrangement in subsequent experiments, the catalyst is run for two hours. This was the time when the sample turned yellow and the red color of the precursor disappeared. In addition to preformation, another ligand can enhance the formation of an active catalyst complex suitable for oxime hydrogenation.

SI 3. Pressure Screening

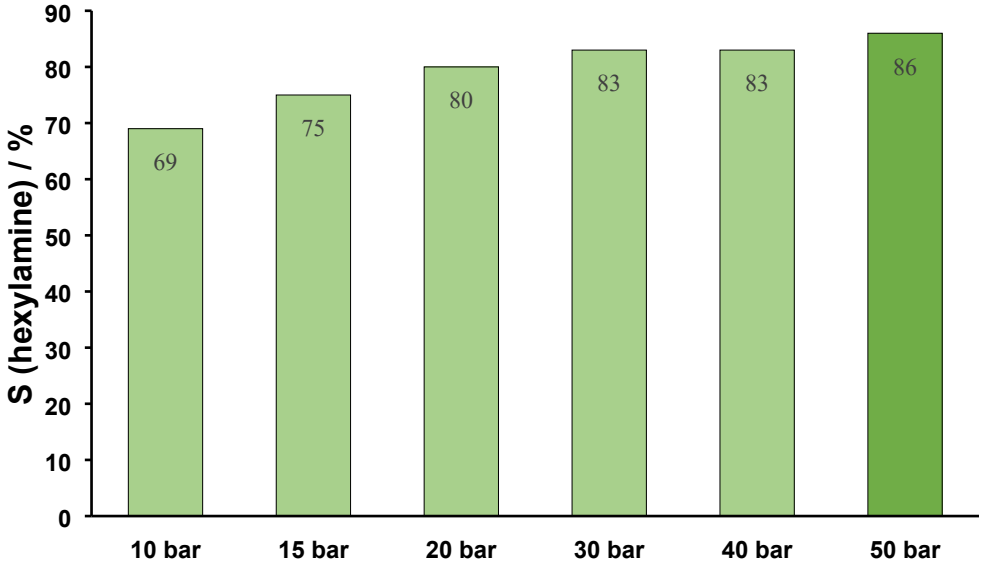

Figure S 3: Screening of the hydrogen pressure. Conditions: 8.33 mmol hexanal oxime (**1a**), 0.5 mol% $Ru(acac)_3$, 0.55 mol% triphos (**L1**), 2.5 mol% KOH, 160 °C, 5 h, 700 rpm, 1,4-dioxane (30 mL). Determined via GC with dodecane as an internal standard.

As expected, higher hydrogen pressure correlates with a higher selectivity of the reaction. Besides the amount of hydrogen, its activation is also crucial for the outcome of the reaction since this is often the rate-limiting step.
A common way to increase the activation of hydrogen is the use of additives. For the selected Ru-triphos system, base or acid additives are usually used. However, under acidic conditions, the oximes tend to undergo a rapid Beckmann rearrangement. Therefore, different bases were investigated for the hydrogenation of aldoximes (see Figure 2).

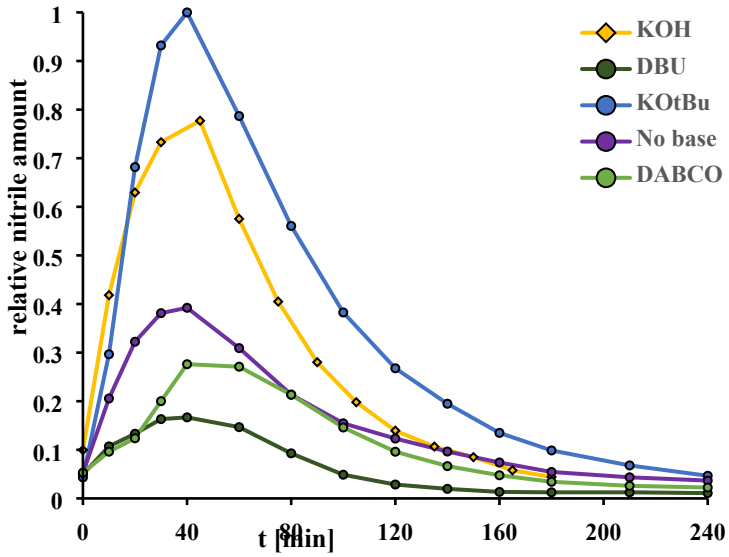

Figure S 4: Relative hexanenitrile (**5a**) amount formed during the hydrogenation with different bases. The highest amount detected with KOH as the reference. Conditions: 8.33 mmol hexanal oxime (**1a**), 0.5 mol% $Ru(acac)_3$, 0.55 mol% triphos (**L1**), 2.5 mol% base, 160 °C, 50 bar H_2, t = 5 h, 700 rpm, 1,4-dioxane (30 mL). Determined via GC with dodecane as an internal standard.

Looking closely at the GC chromatograms, additional signals could be observed when amine bases such as DABCO (**B1**) and DBU (**B2**) were used. To clarify which side products belong to those signals, HPLC-HRMS experiments were carried out. These experiments revealed the formation of two new condensates (Figure S 5) that were not observed using KO*t*Bu (**B3**) and KOH (**B4**). This could hint at a nitrogen-based catalytic step or acid-base reaction taking place at different pH.

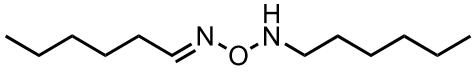

11
Chemical Formula: $C_{12}H_{26}N_2O$
Exact Mass: 214.20
Molecular Weight: 214.35

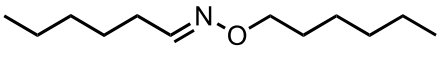

12
Chemical Formula: $C_{12}H_{25}NO$
Exact Mass: 199.19
Molecular Weight: 199.34

Figure S 5: New condensates observed in the hydrogenation of hexanal oxime (**1a**) in the presence of amine bases.

The masses shown in Figure S 5 were found in the measurement for the sample after 5 min, corresponding to the time when there were high intensities of the former unknown signal. The left compound (**11**) can result from the condensation of a hexanal oxime (**1a**) with a hexyl hydroxylamine (**2a**). In contrast, the right compound (**12**) can be built by condensing hexanal oxime (**1a**) with hexanol (**9a**). Both condensate molecules are intermediates in the reaction system since both can be reduced to the desired primary amine (**3a**). However, the oxime ether (**12**) releases an additional hexanol (**9a**) in the process and explains the formation of hexanol (**9a**) when the oxime is already completely converted.

SI 4. Precursor screening

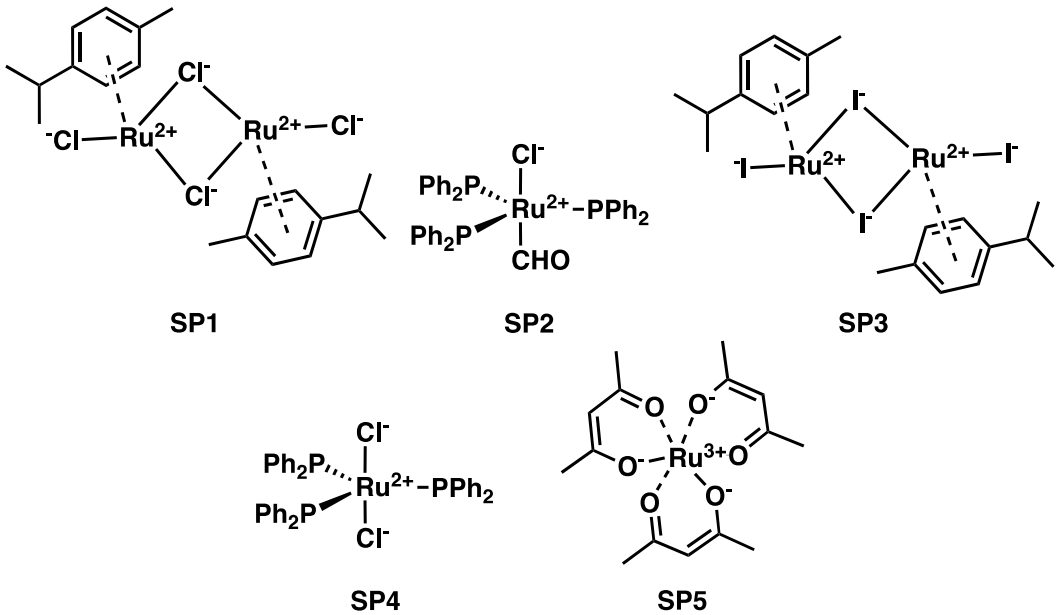

SP1 **SP2** **SP3**

SP4 **SP5**

Figure S 6: Depiction of the tested ruthenium salts.

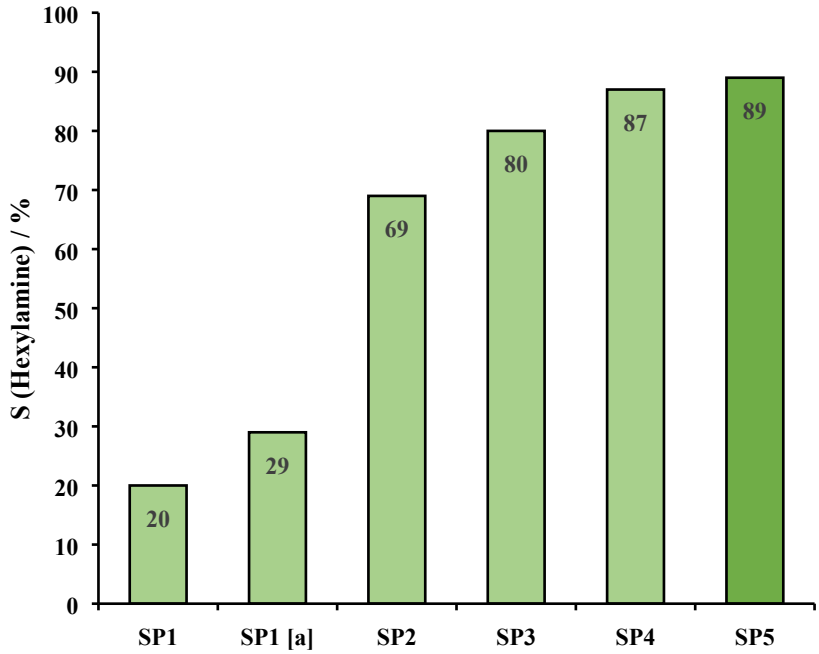

Figure S 7: Precursor screening. Conditions: T = 160 °C, p(H_2) = 50 bar, precursor = 0.5 mol% (Ru), triphos (**L1**) = 0.55 mol%, DBU (**B2**) = 2.5 mol% and hexanal oxime (**1a**) = 8.33 mmol, dioxane (30 mL), t = 5 h, rpm = 700. Selectivity of hexylamine (**3a**) was calculated by GC by using dodecane as an internal standard. [a]: T = 200 °C, dppe = 0.8 mol%, on 25 mmol scale.

The optimization was started with $Ru(acac)_3$ (**SP5**) since this system is also often used in the literature.[3–5]
Additionally, Ru^{II} precursors were tested, which are commonly used for other ruthenium amination reactions.
Surprisingly, **SP2** exhibited a selectivity of only 69 % despite being the preferred precursor for numerous analogous catalyst systems. **SP4** demonstrated a comparable selectivity; however, it led to the accumulation of hexyl hydroxylamine (**2a**) during the reaction, potentially resulting in additional side reactions. The best results were achieved with **SP5,** and the reaction system was not altered after the precursor screening.

SI 5. Solvent screening

Another essential factor for the homogeneous catalyst system is the solvent since it influences the solubility of the catalyst and the substrates. 1,4-Dioxane is an excellent solvent for Ru catalyzed hydrogenation reactions, but it is suspected to cause cancer, making it desirable to find an alternative. Referring to the principles of green chemistry, harmful solvents should be replaced with less dangerous substitutes.
Toluene is also an established solvent that has a stabilizing effect on the catalyst, so it was tested along with anisole. Anisole contains an aromatic ring with a methyl ether, thus combining the structural properties of dioxane and toluene. They were compared in the hydrogenation of hexanal oxime (**1a**) (Figure S 8).

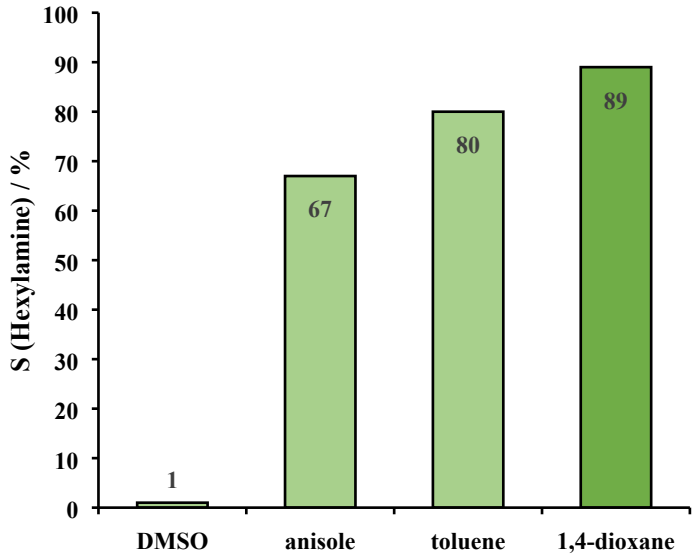

Figure S 8: Solvent screening for the hydrogenation of hexanal oxime (**1a**). Conditions: T = 160 °C, $p(H_2)$ = 50 bar, $Ru(acac)_3$ = 0.5 mol%, triphos (**L1**) = 0.55 mol%, DBU (**B2**) = 2.5 mol% and hexanal oxime (**1a**) = 8.33 mmol, solvent (30 mL), t = 5 h, rpm = 700. Selectivity of hexylamine (**3a**) was calculated by GC by using dodecane as an internal standard.

Despite the additional ether functionality, anisole performed the worst with only 67 % selectivity, and toluene also underperformed dioxane. The structural difference could explain the difference. Both toluene and anisole are aromatic and can coordinate mainly through π-π-interactions, which seems less effective than the coordinating oxygen atoms in dioxane. Moreover, dioxane can act as a bidentate ligand, increasing its stabilizing effect on the catalyst. Hence, the performance of dioxane with 89 % selectivity remains the best.

Hydroformylation at the start of the new reaction sequence

We tested the reaction sequence from the alkene to the primary amine for 1-penten (**10a**), 1-octene (**10d**) and methyl 10-undecenoate (UME) (**10f**). The latter is of high interest since it opens a new synthesis route for polyamide 12 from renewable resources.

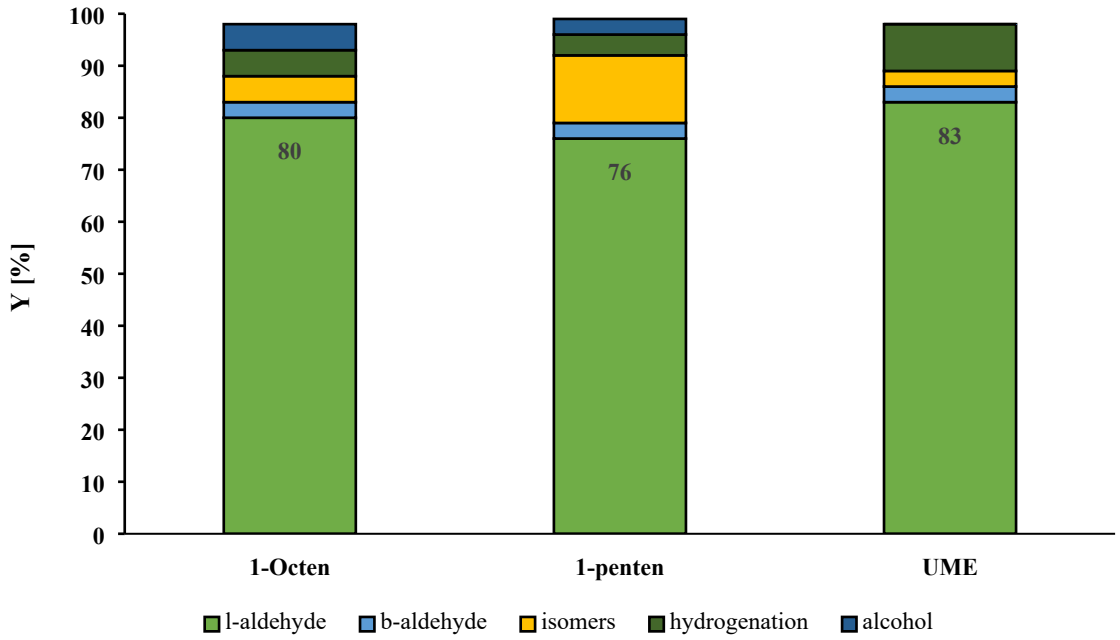

Figure S 9: Performance of the hydroformylation step with the three tested alkenes. Conditions: Hydroformylation: preforming: CO/H_2 (30 bar), n_{CO}/n_{H2} = 1, 12 h, at 120 °C; reaction: 32 mmol of **10,** CO/H_2 (30 bar), n_{CO}/n_{H2} = 1, 6 h, at 120 °C $m_{water}/m_{substrate}$ = 0.2, $n_{substrate}/n_{Rh}$ = 500, n_{CD}/n_{Rh} = 100, n_P/n_{Rh} = 7.

All the alkenes were tested with an aqueous biphasic system to obtain a relatively pure product phase without the rhodium catalyst or additional solvents. Cyclodextrins were added as a phase-transfer agent since the substrates are not soluble in the aqueous catalyst phase.
Starting with 1-octene (**10d**), the hydroformylation reached high yields of nonanal with an l/b ratio of 26.7. The hydroformylation of 1-pentene (**10a**) showed more isomerization but still had a yield of 75 % with an l/b ratio of 25.3. Surprisingly, the best results were achieved with the long-chain UME (**10f**). The yield was 83 %, with an l/b ratio of 27.7.

SI 6. Definition of Productivity

Within our manuscript we have used the term productivity to compare different reaction conditions. Because the reaction network of the aldoxime reduction contains different intermediates, the conversion of the starting material is not meaningful, due to the different reaction speed of these different reaction paths. We suggest to compare the bulit product per catalyst and time as a better comparison for this reaction. Similar to the TOF_{20} the $Productivity_{20}$ is calculated at 20 % yield io avoid the endpoint of the reaction and show the activity of the catalyst during the reaction.

$$Productivity_{20} = \frac{n(product)}{n(catalyst) \times time(for\ 20\ \%\ yield)} \qquad \text{Equation 1}$$

SI 7. General reaction procedure

Oxime hydrogenation in 20 mL autoclave

Hexanal oxime (**1a**) (1 mmol, 1 eq.), metal precursor (0.01 mmol, 0.01 eq.), ligand (0.02 mmol, 0.02 eq.) and the base (Na_2CO_3, K_2CO_3 as solid; NaOH, KOH, KO*t*Bu as solution in water/dioxane) were weighed into multiplex reactors. The reactors

were closed, flushed with argon, and degassed solvent (2 mL) was added. The reactors were gassed with hydrogen at 10 bar and stirred at 160 °C for 18 hours. The reactors were opened, and 1 mL of the solution was analyzed by GC/FID or GC/MS.
The internal standard was added either after solvent addition before the reaction or after the reaction in the same GC vial.

Oxime hydrogenation in 100 mL autoclave

First, the reactor was equipped with a stirring bar and then tightly closed. Then, KO*t*Bu **B3** / 1,4-dioxane stock solution was prepared (0.00832 mmol/mL), and this was degassed under argon atmosphere in an ultrasonic bath. $Ru(acac)_3$ (16.6 mg, 0.0417 mmol, 0.005 eq.) and the ligand **L1**-**L7** (see Figure 1) were placed in another Schlenk flask and then dissolved in 25 mL of the degassed base/solvent solution. The reactor was evacuated and purged with argon and vacuum was used to pull the catalyst and ligand solution into the reactor *via* the sampling valve. During this, the hexanal oxime (**1a**) (8.33 mmol, 959 mg, 1 eq.) was dissolved in 5 mL of solvent and degassed for 1 h. Then, the oxime solution was filled into the dropping funnel with a syringe under argon counterflow. Then, the reactor was gassed with 30 bar of hydrogen and heated to 160 °C internal temperature, and the catalyst was allowed to preform for 2 h while stirring. At the end of the 2 h, the oxime was added *via* the dropping funnel, and the first sample was taken.
Samples were prepared *via* the sampling valve into GC vials, which were frozen in liquid nitrogen. The collected sample volume was then weighed and prepared for GC measurements using dodecane as an external standard and 2-propanol as solvent.

Oxime hydrogenation in 300 mL autoclave

In a Schlenk flask under argon atmosphere, $Ru(acac)_3$ **SP5** (49.8 mg, 0.125 mmol, 0.005 eq.) and triphos **L2** (88.6 mg, 0.138 mmol, 0.0055 eq.) were weight in. The flask was flushed with argon before dioxane (65 ml) was added. Then DBU (**B2**) (97 mg, 0.625 mmol, 0.025 eq.) was added through a septum and the mixture was mixed.
A 300 mL overhead stirred pressure autoclave was purged with argon. Vacuum was pulled on the reactor, and the catalyst mixture was transferred in the reactor through a teflon tube attached to the sampling valve utilizing the low pressure inside. The oxime (25 mmol, 1 eq.) was weighed in a separate Schlenk flask under argon atmosphere and dissolved in 35 mL dioxane. The substrate mixture was transferred into a pressure-dropping funnel mounted to the reactor *via* a syringe under an argon flow. The reactor was charged with 50 bar H_2 and heated to 200 °C (80 bar pressure at reaction temp.). The catalyst was preformed for 2 h, stirring at 750 rpm with a gas-inlet stirrer. After the preforming period, the dropping funnel was opened, and the reaction started. Samples were drawn after 1, 5.30, 10.30, 15, 20, 30, 40, and 60 min and analyzed *via* GC using dodecane as the internal standard.

Oximation of aldehydes

Hydroxylamine solution (50 % aq., 144 mmol, 1.44 eq.) was placed in a 3-neck flask equipped with a dropping funnel. The dropping funnel was charged with the corresponding aldehyde (100 mmol, 1 eq.).

The flask was cooled to 0 °C in an ice bath, and the solution was stirred with 600 rpm. The aldehyde was added dropwise to the solution. 5 mL of water were used to rinse the addition funnel. After the addition was completed, HCl (conc., 0.01 eq.) was added, the reaction mixture was allowed to warm up to rt, and the stirring speed was increased to 900 rpm.
The mixture was extracted with diethyl ether 3 times. The organic phases were combined, and the solvent was removed under reduced pressure.

Oximation of hydroformylation reaction solution

Starting with a hydroformylation reaction solution (145 g) in *I*-butanol with a 60.4 wt% aldehyde 1.1 eq. Hydroxylamine as a 50 wt% aqueous solution was added slowly at 0 °C before adding conc. HCl (0.1 mol%) *via* a 1 ml syringe. Following the addition of the acid, the reaction was allowed to warm to rt and was stirred overnight to ensure reaction completion. Subsequently, the solids that had formed were filtered off, washed with water, and then rinsed with pentane. After the washes, the solid precipitate was dried under reduced pressure to remove any residual solvents or impurities.
Another filtration step was conducted to improve the yield. Additional product was further precipitated by adding water to the filtrate.

Synthesis of hexanamide (4a)

Hexanal oxime (**1a**) (1 mmol, 1 eq.), $Ru(acac)_3$ **SP5** (0.01 mmol, 0.01 eq.), triphos **L2** (0.02 mmol, 0.02 eq.) and KOH (**B4**) (0.025 mmol, 0.02 mmol) were weighed into a 20 mL reactor. The reactor was closed, flushed with argon, and degassed 1,4-dioxane (2 mL) was added. The reactor stirred at 160 °C for 18 hours. The reactor was opened, and 1 mL of the solution was analyzed by GC/FID and GC/MS. The remaining solution was united with the sample solution, and the solvent was evaporated by a rotary evaporator, yielding a brown oil. The oil was worked up by column chromatography with pure ethyl acetate, yielding the hexanamide as an off-white solid (44 mg, 0.38 mmol, 38 %).

SI 8. Analytics:

^{1}H NMR & ^{13}C NMR:

All samples were measured in the workgroup of PROF. DR. HILLER.
Spectrometer: Bruker Avance III HD NanoBay - 400 MHz, Bruker Avance NEO – 500 MHz, Bruker Avance III HD – 600 MHz, Agilent DD2 - 500 MHz.
Internal standards (^{1}H NMR): $CDCl_3$ (δ = 7.26 ppm).
The number of hydrogen atoms per signal was determined by comparing the integrals.
Hydrogen atoms of the E/Z-Isomers are nominated as E/Z 1H.
Internal standards (^{13}C NMR): $CDCl_3$ (δ = 77.0 ppm).
The number of carbon atoms per signal was determined by comparing the integrals.

HPLC-HRMS

All samples were measured in the workgroup of DR. ZÜHLKE.

For the HPLC separation, the following system was used: system (Agilant 1200-series) comprising: autosample (G1367B HiPALS), pump (G1312B Binary Pump SL), column oven (G1316B TCC SL) and PDA detector (G1315C DAD SL), degaser (G1379B) with a Nucleoshell RP 18, 2.7 µm, 100 x 3 mm column.
For the mass analysis, a Mass spectrometer LTQ-Orbitrap manufactured by Thermo Fischer Scientific was used. Additionally, a Bruker compact time of flight mass analyzer was used.

Compound characterization

Hexanal oxime (1a)

^{1}H NMR (600 MHz, $CDCl_3$) δ = 9.35 (s, 1H), 7.40 (t, *J* = 6.2 Hz, *E*/*Z* 1H), 6.70 (t, *J* = 5.5 Hz, *E*/*Z* 1H), 2.36 (td, *J* = 7.6, 5.4 Hz, 1H), 2.17 (td, *J* = 7.6, 6.2 Hz, 1H), 1.52 – 1.42 (m, 2H), 1.35 – 1.25 (m, 4H), 0.92 – 0.83 (m, 3H).

E/Z: 1:1.08

^{13}C NMR (151 MHz, $CDCl_3$) δ = 153.00, 152.45, 31.63, 31.32, 29.52, 26.36, 25.80, 25.07, 22.44, 14.01, 14.00.

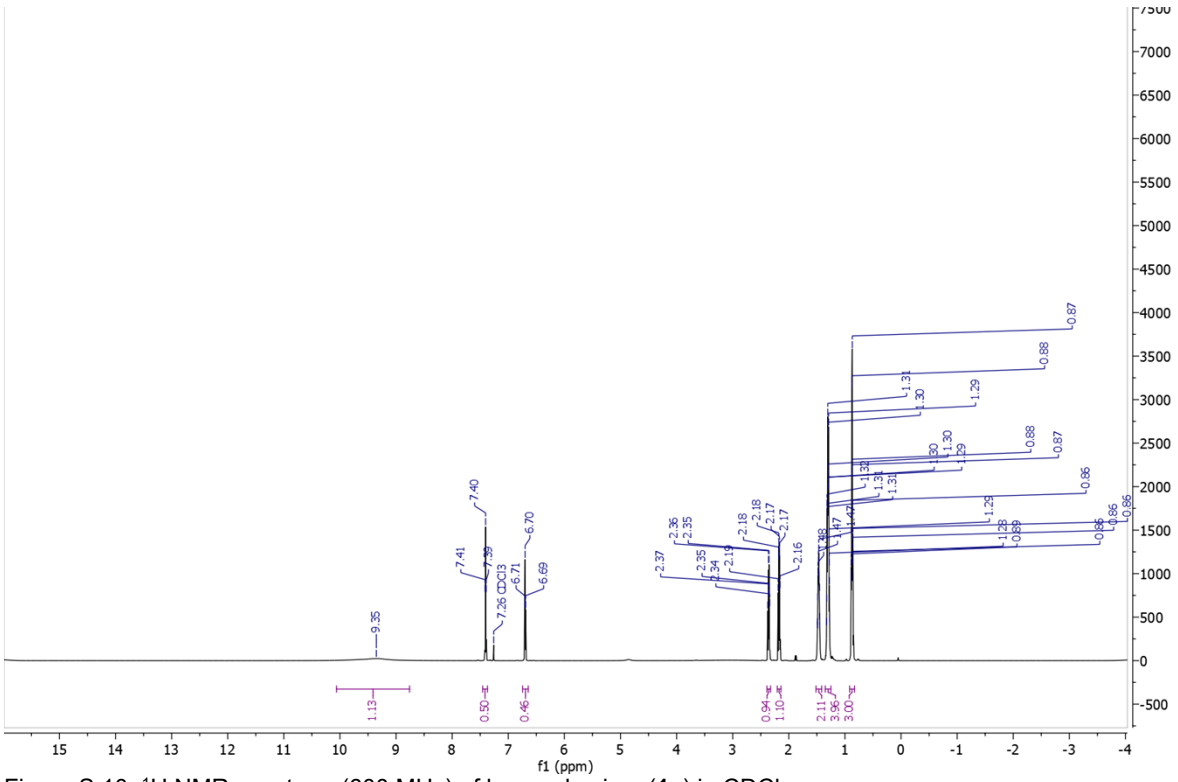

Figure S 10: ^{1}H NMR spectrum (600 MHz) of hexanal oxime (**1a**) in $CDCl_3$.

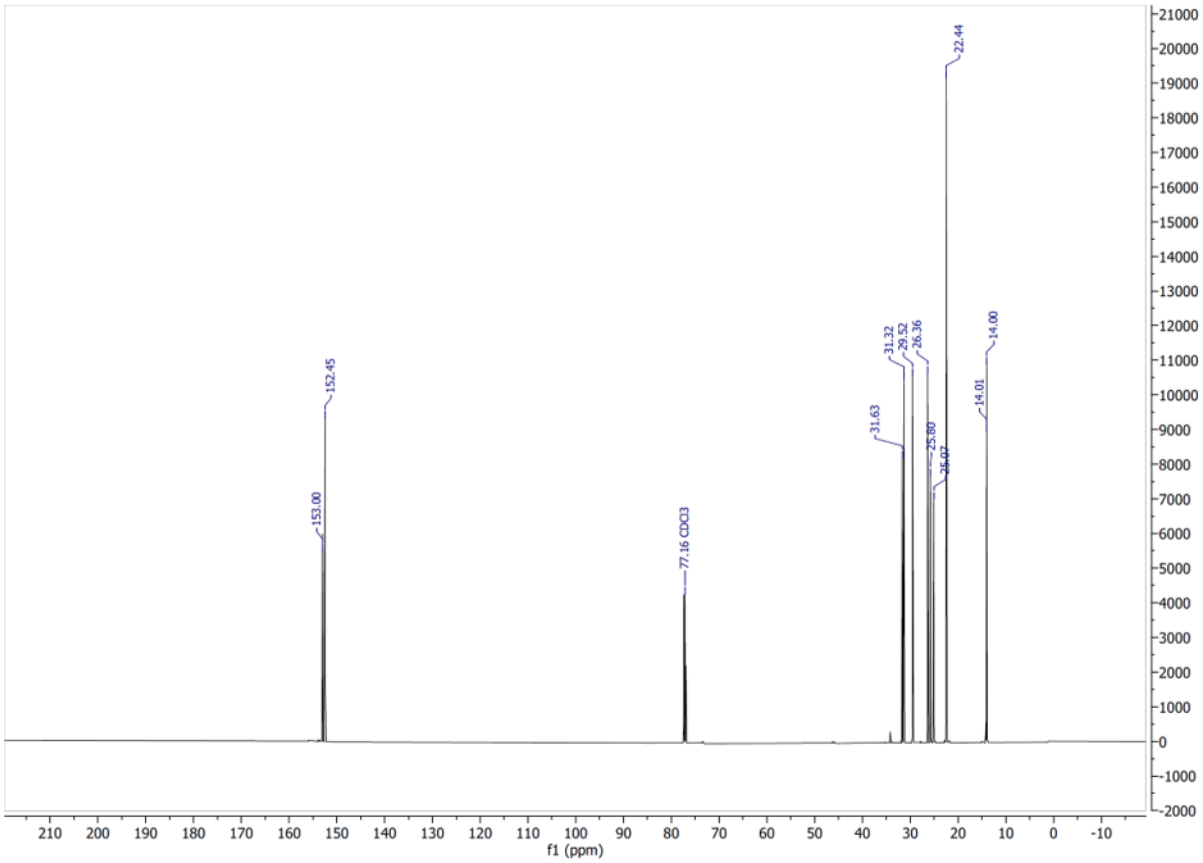

Figure S 11: ^{13}C NMR spectrum (151 MHz) of hexanal oxime (**1a**) in $CDCl_3$.

LC-HRMS of hexanal oxime (**1a**) ($C_6H_{13}NO$) $[M+H]^+$: calculated: 116.1070; detected: 116.1071 (-1.3 ppm deviation).

LC-HRMS of hexyl hydroxylamine (**2a**) ($C_6H_{15}NO$) $[M+H]^+$: calculated 118.1226; detected: 118.1228 (-1.3 ppm deviation).

LC-HRMS of hexylamine (**3a**) ($C_6H_{15}N$) $[M+H]^+$: calculated 102.1277; detected: 102.1280 (-2.9 ppm deviation).

LC-HRMS of hexanenitrile (**5a**) ($C_6H_{11}N$) $[M+H]^+$: calculated 98.0964; detected: 98.0961 (2.8 ppm deviation).

LC-HRMS of hexylimine (**6a**) ($C_6H_{13}N$) $[M+H]^+$: calculated 100.1121; detected: 100.1118 (-2.5 ppm deviation).

LC-HRMS of dihexylamine (**7a**) ($C_{12}H_{27}N$) $[M+H]^+$: calculated 186.2216; detected: 186.2222 (-2.9 ppm deviation).

LC-HRMS of dihexylimine ($C_{12}H_{25}N$) $[M+H]^+$: calculated 184.2060; detected: 184.2065 (-2.7 ppm deviation).

Hexanamide (4a):

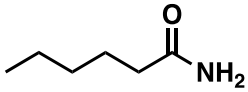

^{1}H NMR (400 MHz, $CDCl_3$) δ = 0.87 - 0.94 (m, 3 H), 1.28 - 1.38 (m, 4 H), 1.64 (q, 2 H), 2.22 (t, 2 H), 5.62 (d, 2 H) ppm.

^{13}C NMR (101 MHz, $CDCl_3$) δ = 13.92, 22.39, 25.23, 31.40, 35.94, 175.81 ppm.

Butanal oxime (1b)

^{1}H NMR (400 MHz, $CDCl_3$) δ = 8.88 (s, *E/Z* 1H), 8.48 (s, *E/Z* 1H), 7.42 (t, *J* = 6.1 Hz, *E/Z* 1H), 6.72 (t, *J* = 5.4 Hz, *E/Z* 1H), 2.36 (td, *J* = 7.5, 5.5 Hz, 1H), 2.18 (td, *J* = 7.4, 6.1 Hz, 1H), 1.53 (q, *J* = 7.4 Hz, 2H), 0.96 (q, *J* = 7.3 Hz, 3H).

E/Z = 1:1.06

^{13}C NMR (101 MHz, $CDCl_3$) δ = 152.95, 152.30, 31.55, 27.01, 20.04, 19.57, 14.01, 13.73.

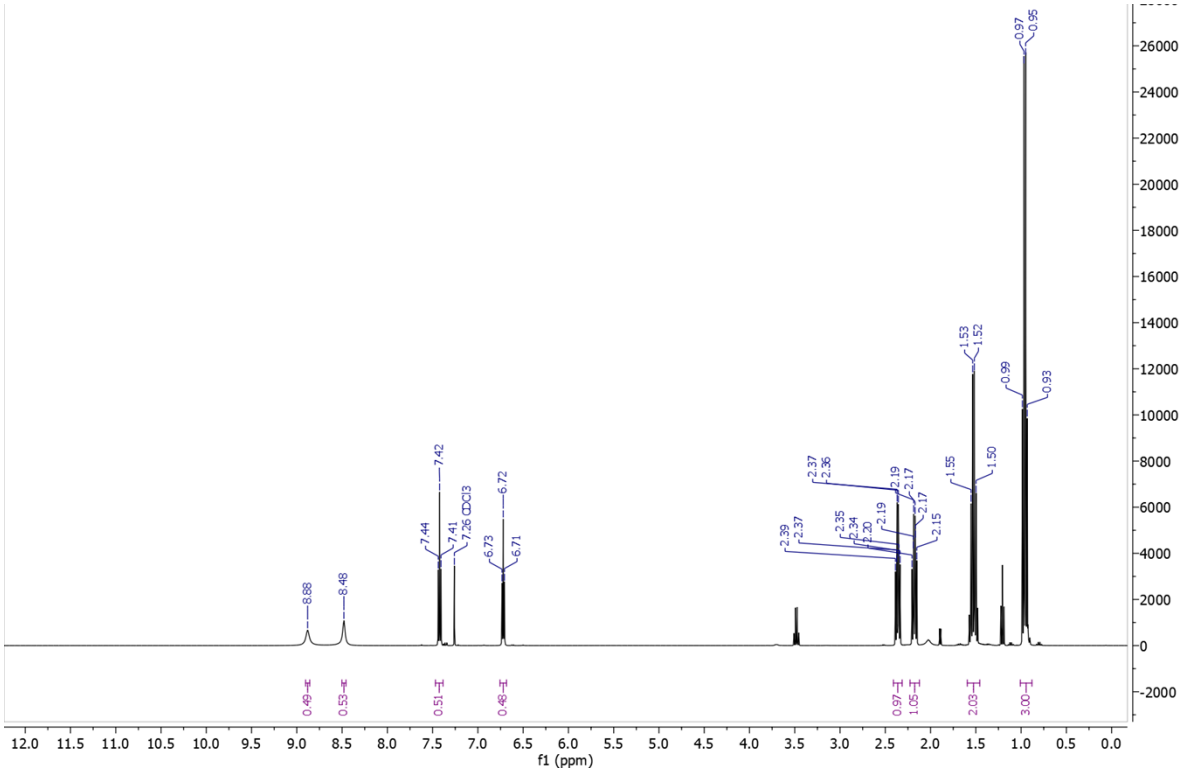

Figure S 12: ^{1}H NMR spectrum (400 MHz) of butanal oxime (**1b**) in $CDCl_3$.

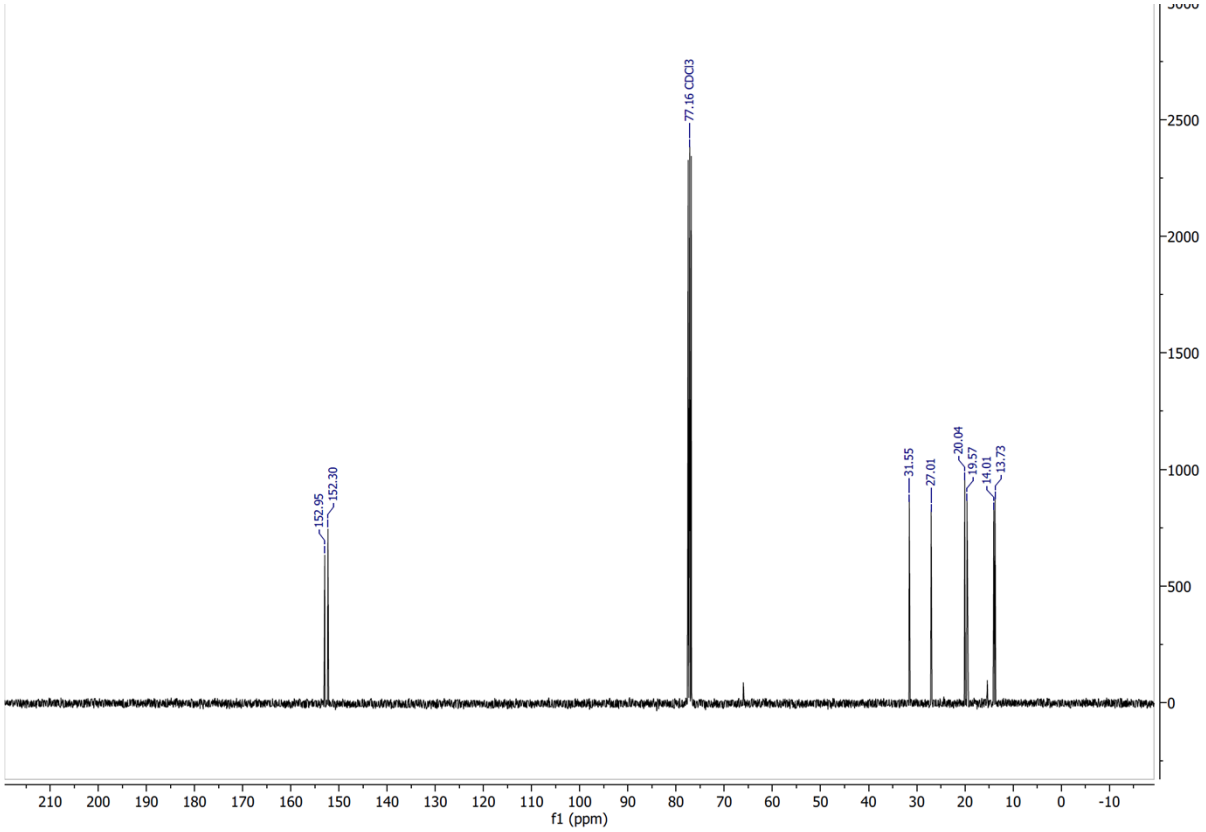

Figure S 13: ^{13}C NMR spectrum (101 MHz) of butanal oxime (**1b**) in $CDCl_3$.

2-Methylpentanal oxime (1c)

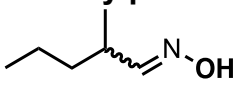

^{1}H NMR (400 MHz, $CDCl_3$) δ = 8.24 (s, 1H), 7.29 (d, *J* = 7.0 Hz, *E/Z* 1H), 6.50 (d, *J* = 7.8 Hz, *E/Z* 1H), 3.15 (p, *J* = 7.1 Hz, *E/Z* 1H), 2.38 (qd, *J* = 7.0, 5.6 Hz, *E/Z* 1H), 1.48 – 1.26 (m, 4H), 1.05 (dd, *J* = 13.3, 6.8 Hz, 3H), 0.96 – 0.85 (m, 3H).

^{13}C NMR (101 MHz, $CDCl_3$) δ = 157.66, 156.73, 36.97, 36.92, 34.27, 29.38, 20.54, 20.27, 18.06, 17.58, 14.17, 14.12.

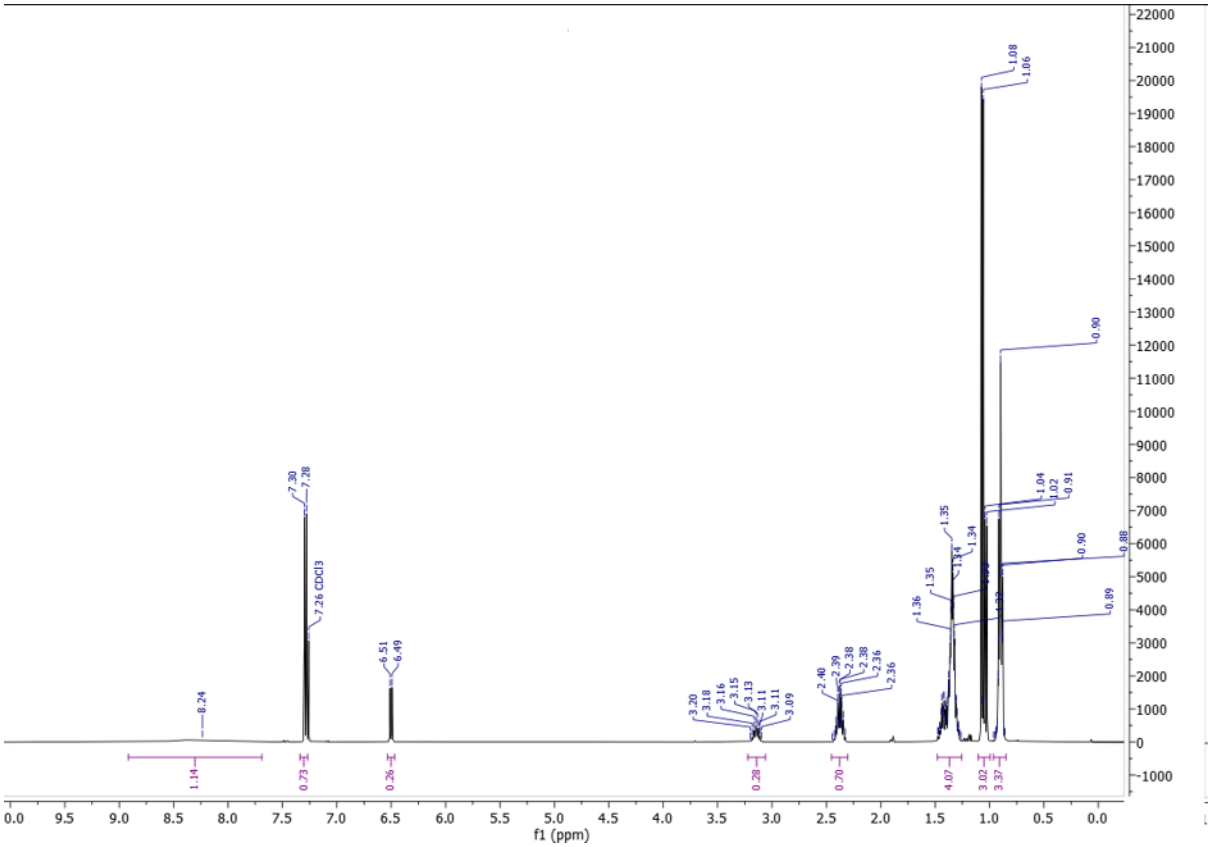

Figure S 14: ^{1}H NMR spectrum (400 MHz) of 2-methylpentanal oxime (**1c**) in $CDCl_3$.

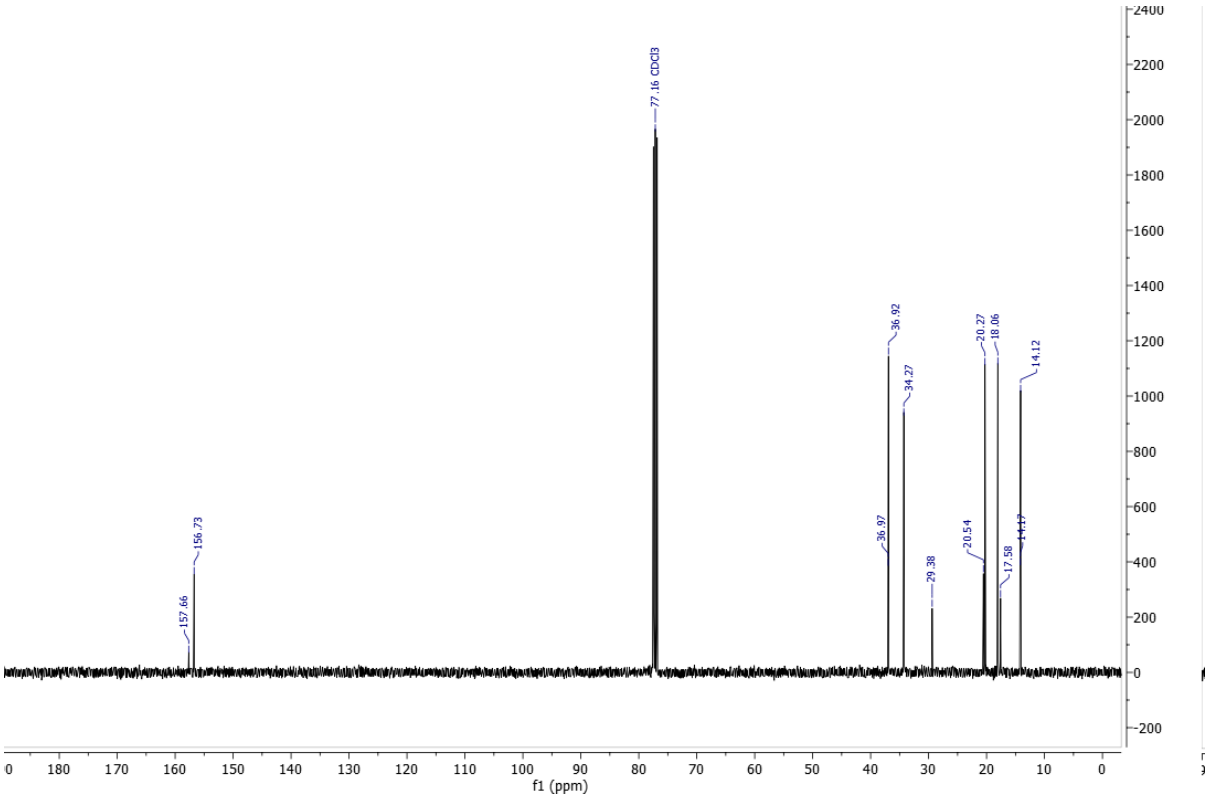

Figure S 15: ^{13}C NMR spectrum (101 MHz) of 2-methylpentanal oxime (**1c**) in $CDCl_3$.

2-Methylpentylamin (3c)

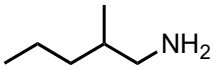

^{1}H NMR (600 MHz, $CDCl_3$) δ = 8.35 (s, 4H), 2.99 – 2.91 (m, 1H), 2.81 – 2.71 (m, 1H), 1.99 – 1.88 (m, 1H), 1.71 (s, 2H), 1.45 – 1.34 (m, 2H), 1.34 – 1.26 (m, 1H), 1.26 – 1.19 (m, 1H), 1.07 (d, *J* = 6.7 Hz, 3H), 0.91 (t, *J* = 7.0 Hz, 3H).

^{13}C NMR (151 MHz, $CDCl_3$) δ = 45.68, 36.26, 31.60, 19.74, 17.53, 14.18.

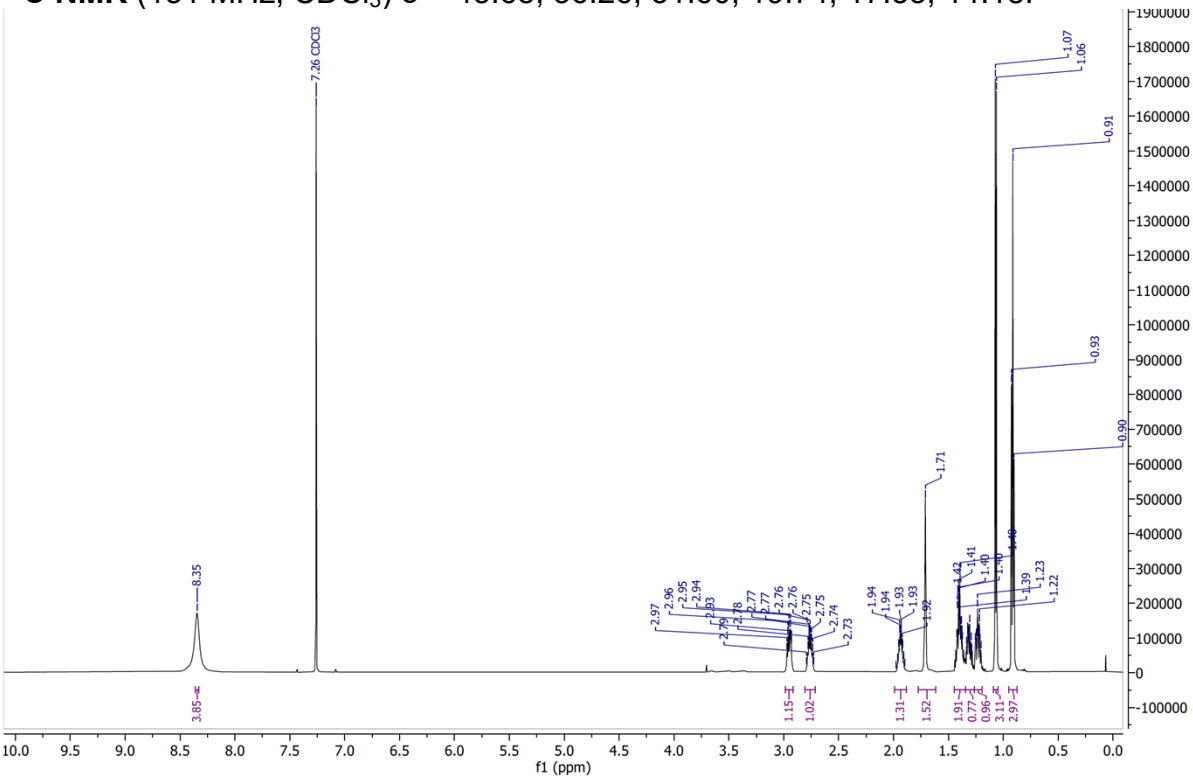

Figure S 16: ^{1}H NMR spectrum (600 MHz) of 2-methylpentylamine (**3c**) in $CDCl_3$.

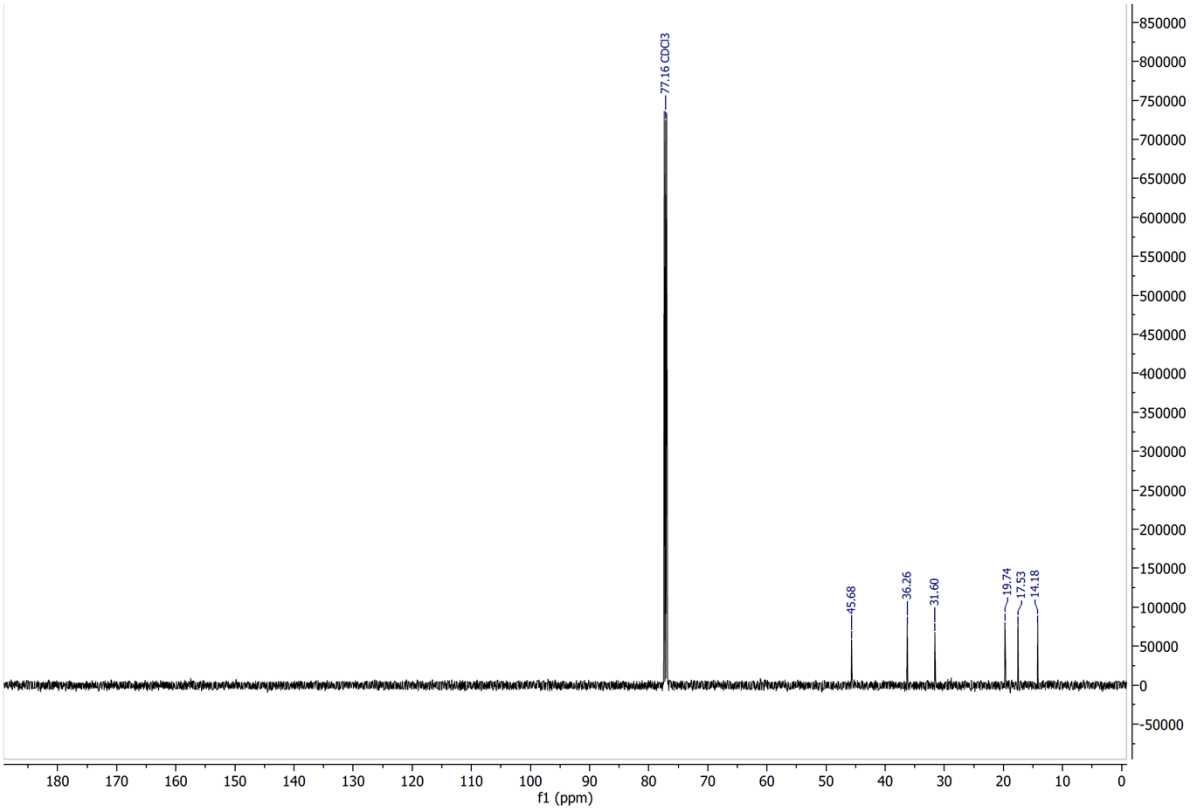

Figure S 17: ^{13}C NMR spectrum (151 MHz) of 2-methylpentylamine (**3c**) in $CDCl_3$.

Nonanal oxime (1d)

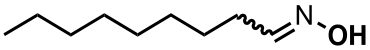

^{1}H NMR (500 MHz, $CDCl_3$) δ = 7.42 (t, *J* = 6.1 Hz, *E/Z* 1H), 6.72 (t, *J* = 5.4 Hz, *E/Z* 1H), 2.37 (td, *J* = 7.6, 5.4 Hz, 1H), 2.19 (td, *J* = 7.6, 6.2 Hz, 1H), 1.52 – 1.44 (m, 2H), 1.38 – 1.19 (m, 10H), 0.88 (td, *J* = 7.0, 1.5 Hz, 3H).

E/Z = 1:1.31

^{13}C NMR (126 MHz, $CDCl_3$) δ = 153.26, 152.58, 77.41, 77.16, 76.91, 31.96, 29.63, 29.52, 29.42, 29.32, 29.30, 29.24, 26.66, 26.19, 25.08, 22.79, 14.24.

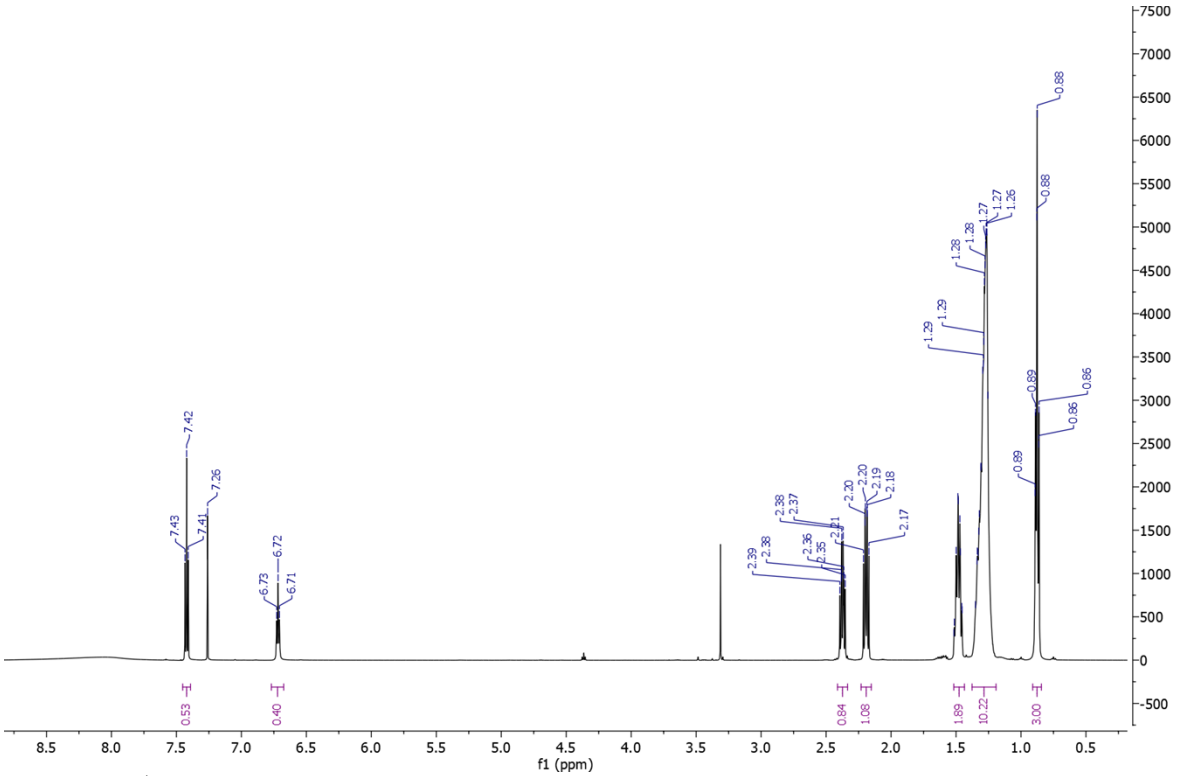

Figure S 18: ^{1}H NMR spectrum (500 MHz) of nonanal oxime (**1d**) in $CDCl_3$.

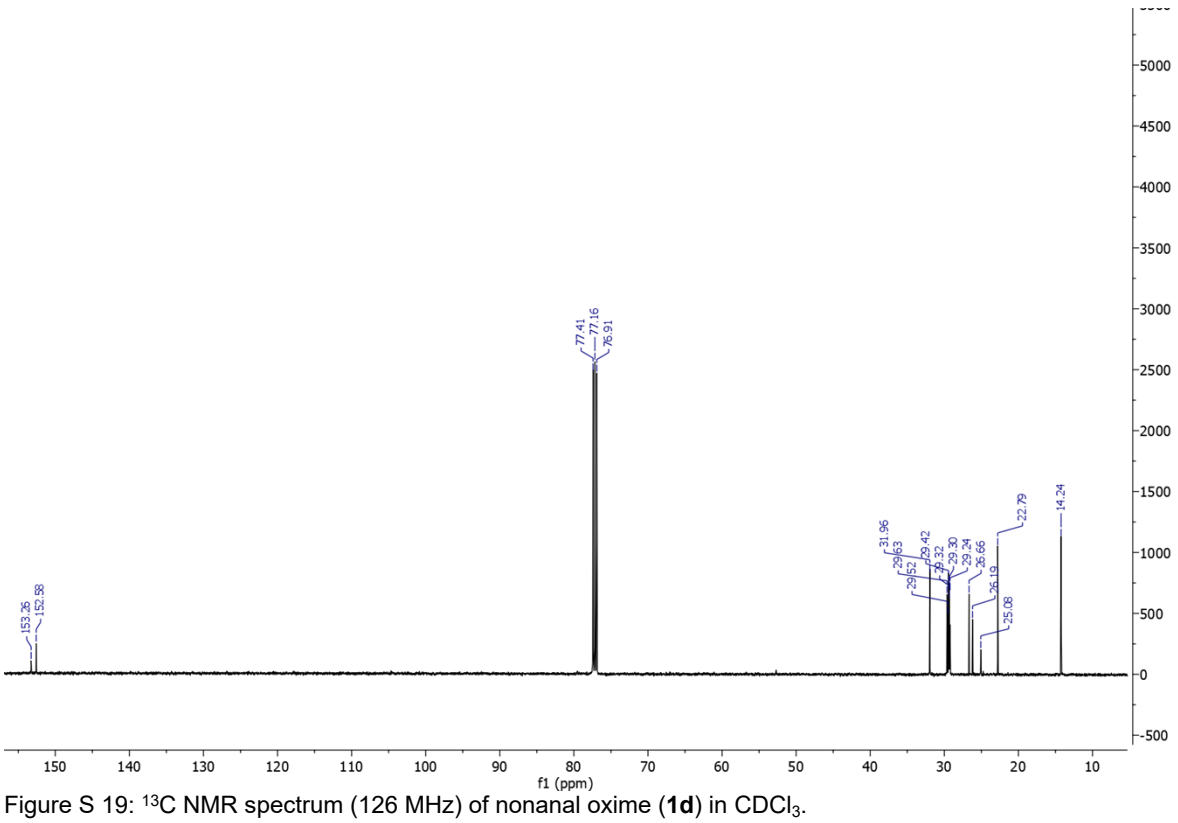

Figure S 19: ^{13}C NMR spectrum (126 MHz) of nonanal oxime (**1d**) in $CDCl_3$.

Nonylamine (3d)

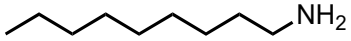

LC-HRMS of nonylamine (**3d**) ($C_9H_{21}N$) $[M+H]^+$: calculated 144.1747; detected: 144.1751 (-3.2 ppm deviation).

Citronellal oxime (1e)

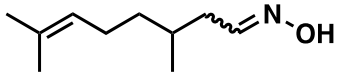

^{1}H NMR (400 MHz, $CDCl_3$) δ = 8.74 (s, 1H), 8.36 (s, 1H), 7.42 (t, *J* = 6.5 Hz, 1H), 6.74 (t, *J* = 5.5 Hz, 1H), 5.08 (dddq, *J* = 7.2, 5.8, 2.9, 1.5 Hz, 2H), 2.43 – 2.16 (m, 3H), 2.10 – 1.89 (m, 5H), 1.68 (t, *J* =1.3 Hz, 7H), 1.60 (t, *J* =1.2 Hz, 7H), 1.36 (dd, *J* = 6.7, 5.7 Hz, 1H), 1.30 – 1.16 (m, 2H), 0.94 (dd, *J* = 7.7, 6.7 Hz, 7H).

^{13}C NMR (101 MHz, $CDCl_3$) δ = 152.15, 151.69, 131.68, 124.49, 124.44, 36.98, 36.78, 36.56, 32.07, 31.06, 30.65, 25.85, 25.61, 25.55, 19.87, 19.58, 17.79.

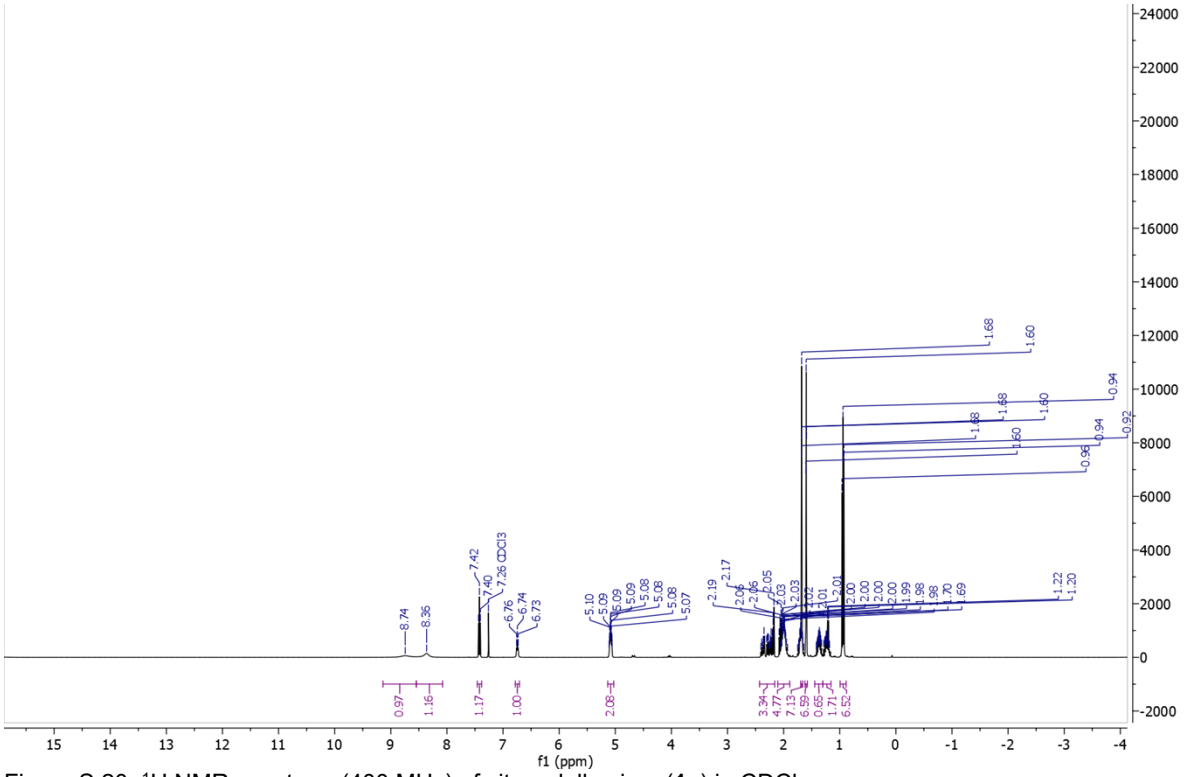

Figure S 20: ^{1}H NMR spectrum (400 MHz) of citronelall oxime (**1e**) in $CDCl_3$.

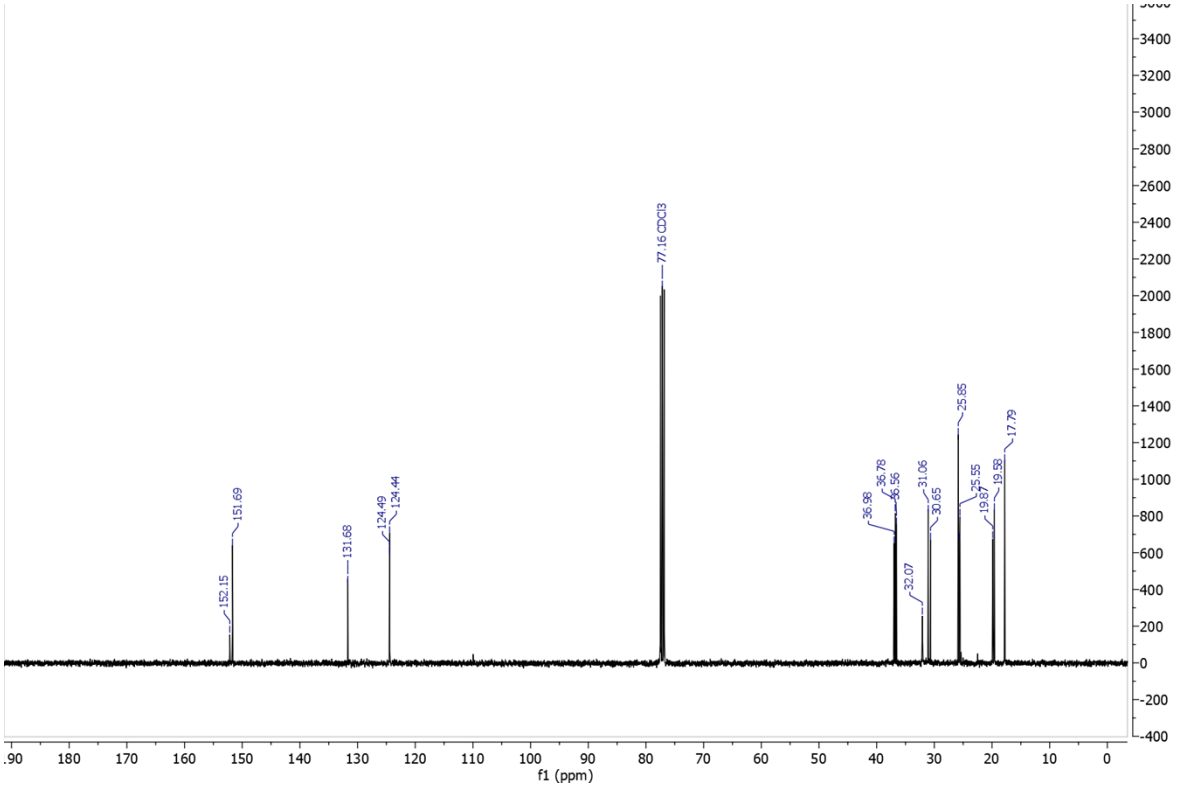

Figure S 21: ^{13}C NMR spectrum (101 MHz) of citronelall oxime (**1e**) in $CDCl_3$.

3,7-dimethyloct-6-en-1-amine (3e)

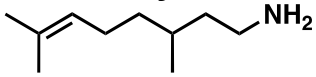

^{1}H NMR (600 MHz, $CDCl_3$) δ = 5.09 (ddp, *J* = 8.4, 5.8, 1.4 Hz, 1H), 3.47 (qd, *J* = 7.0, 0.9 Hz, 2H), 2.77 – 2.62 (m, 2H), 2.04 – 1.89 (m, 2H), 1.67 (s, 2H), 1.60 (s, 2H), 1.54 – 1.41 (m, 2H), 1.36 – 1.22 (m, 2H), 1.22 – 1.18 (m, 3H), 0.92 – 0.84 (m, 3H).

^{13}C NMR (151 MHz, $CDCl_3$) δ = 131.31, 124.96, 65.99, 41.36, 40.25, 37.36, 30.28, 25.85, 25.63, 19.69, 17.78, 15.41.

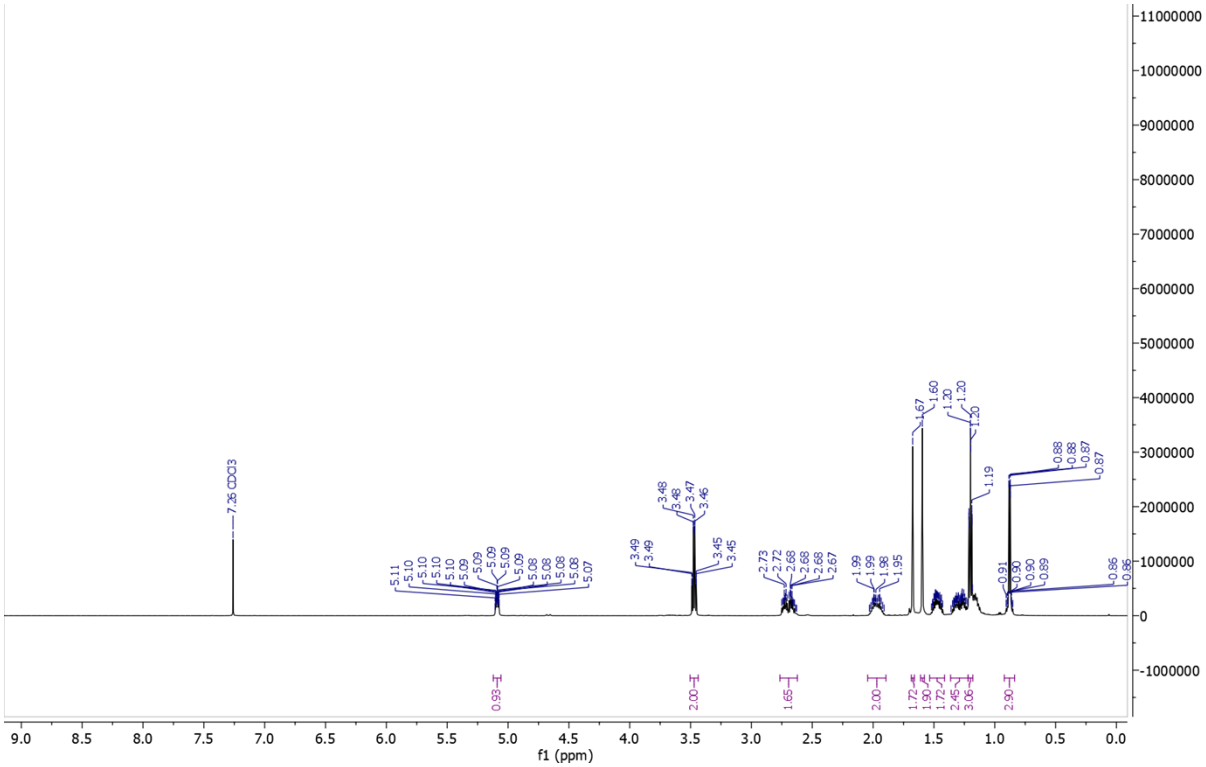

Figure S 22: ^{1}H NMR spectrum (600 MHz) of citronelyl amin (**3e**) in $CDCl_3$.

LC-HRMS of 3,7-dimethyloct-6-en-1-amine ($C_{10}H_{22}N$) $[M+H]^+$: calculated 156.17075; detected: 156.1745 (-1.32 ppm deviation).

3,7-dimethyloctan-1-amine (3e')

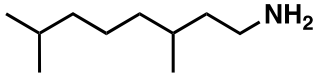

LC-HRMS of 3,7-dimethyloctan-1-amine ($C_{10}H_{24}N$) $[M+H]^+$: calculated 158.18640; detected: 158.1900 (-1.8847 ppm deviation)

Methyl-12-oxododecanoate oxime (1f)

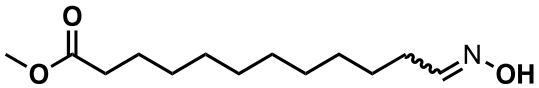

^{1}H NMR (600 MHz, $CDCl_3$) δ = 7.56 (s, *E*/*Z* 1H), 7.42 (t, *J* = 6.1 Hz, *E*/*Z* 1H), 7.25 (s, *E*/*Z* 1H), 6.71 (t, *J* = 5.5 Hz, *E*/*Z* 1H), 3.67 (s, 3H), 2.37 (td, *J* = 7.6, 5.5 Hz, 1H), 2.30 (t, *J* = 7.6 Hz, 2H), 2.19 (td, *J* = 7.5, 6.1 Hz, 1H), 1.65 – 1.57 (m, 5H), 1.36 – 1.25 (m, 12H).

E/Z: 3.19:1

^{13}C NMR (151 MHz, $CDCl_3$) δ = 174.55, 153.42, 152.68, 51.61, 34.26, 29.54, 29.52, 29.50, 29.47, 29.45, 29.35, 29.33, 29.25, 29.15, 26.63, 26.20, 25.08, 24.96.

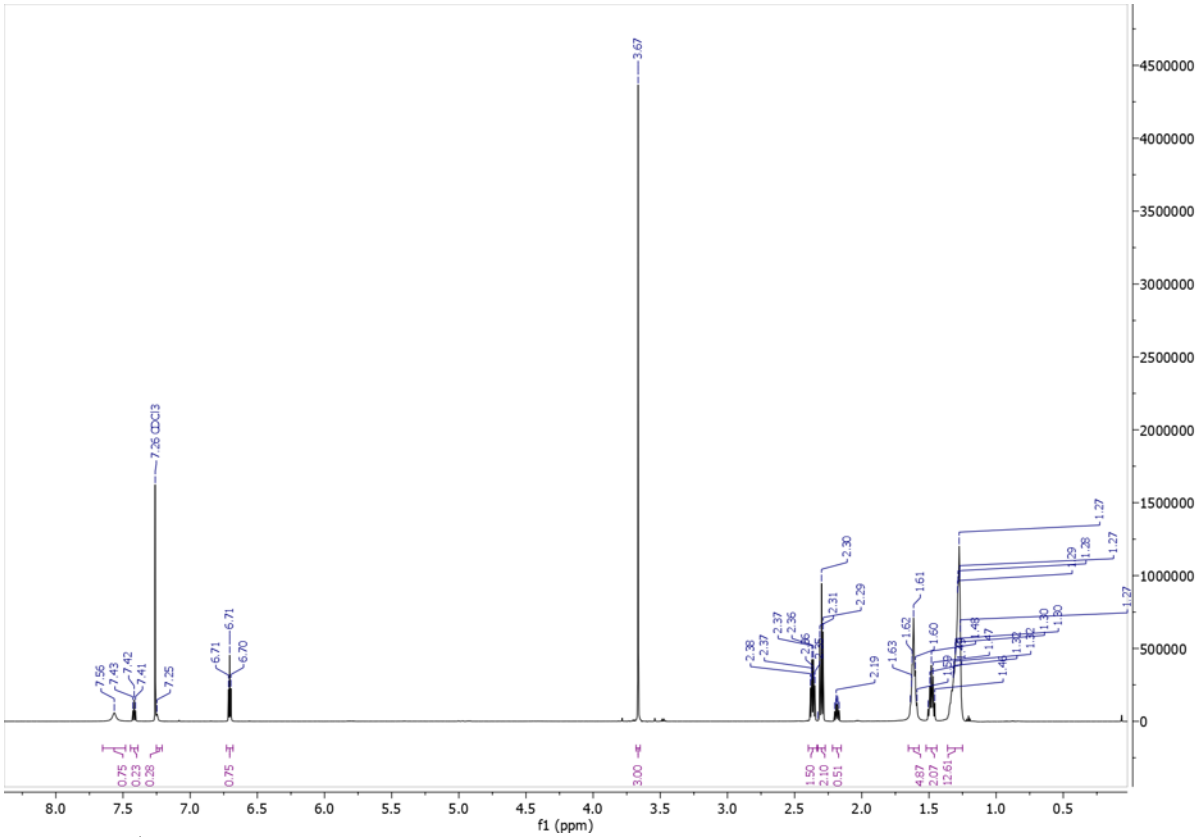

Figure S 23:[1]H NMR spectrum (600 MHz) of methyl-12-oxododecanoate oxime (**1f**) in $CDCl_3$.

Methyl 12-oxododecanoate (8f)

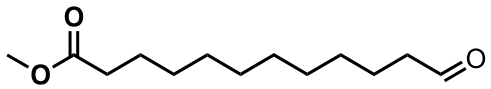

[1]H NMR (400 MHz, C_6D_6) δ = 9.34 (t, *J* = 1.7 Hz, 1H), 3.37 (s, 3H), 2.13 (t, *J* = 7.4 Hz, 2H), 1.83 (td, *J* = 7.3, 1.7 Hz, 2H), 1.57 (t, *J* = 7.3 Hz, 2H), 1.31 (p, *J* = 7.3 Hz, 2H), 1.24 – 1.00 (m, 12H).

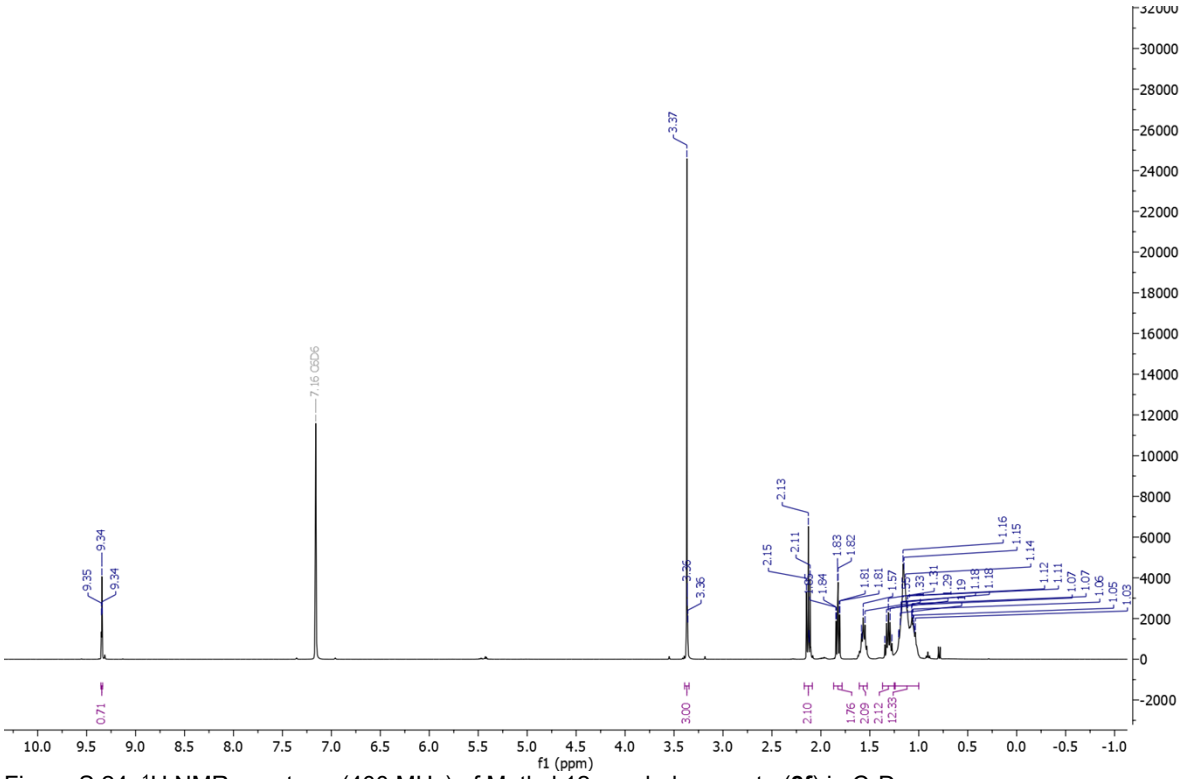

Figure S 24: ^{1}H NMR spectrum (400 MHz) of Methyl 12-oxododecanoate (**8f**) in C_6D_6.

Methyl 12-aminododecanoate (**3f**)

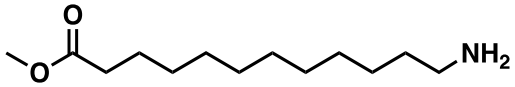

^{1}H NMR (500 MHz, $CDCl_3$) δ = 3.65 (s, 3H), 2.68 – 2.62 (m, 2H), 2.28 (t, *J* = 7.6 Hz, 2H), 1.58 (dt, *J* = 15.1, 7.4 Hz, 2H), 1.44 – 1.38 (m, 2H), 1.29 – 1.23 (m, 14H).

^{13}C NMR (151 MHz, $CDCl_3$) δ = 174.49, 51.58, 42.43, 34.26, 34.06, 29.73, 29.66, 29.63, 29.56, 29.38, 29.28, 27.04, 25.10.

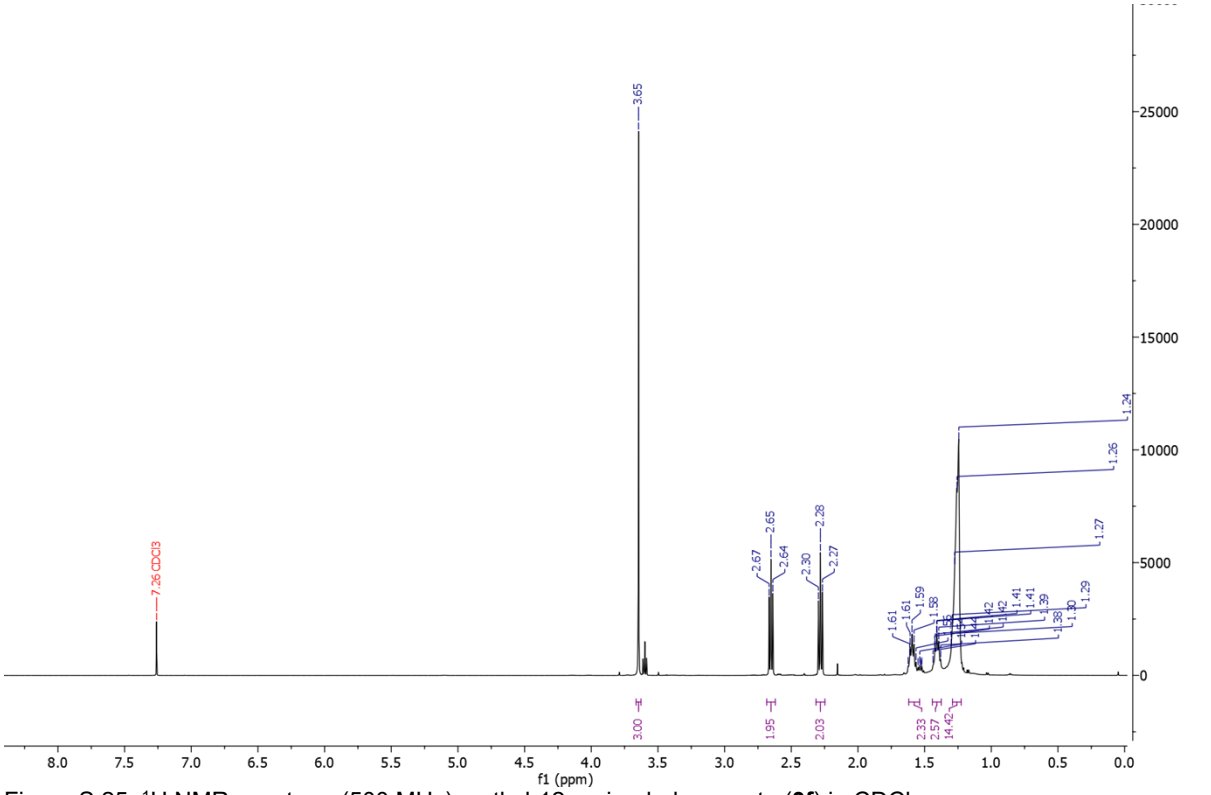

Figure S 25: ^{1}H NMR spectrum (500 MHz) methyl-12-aminododecanoate (**3f**) in $CDCl_3$.

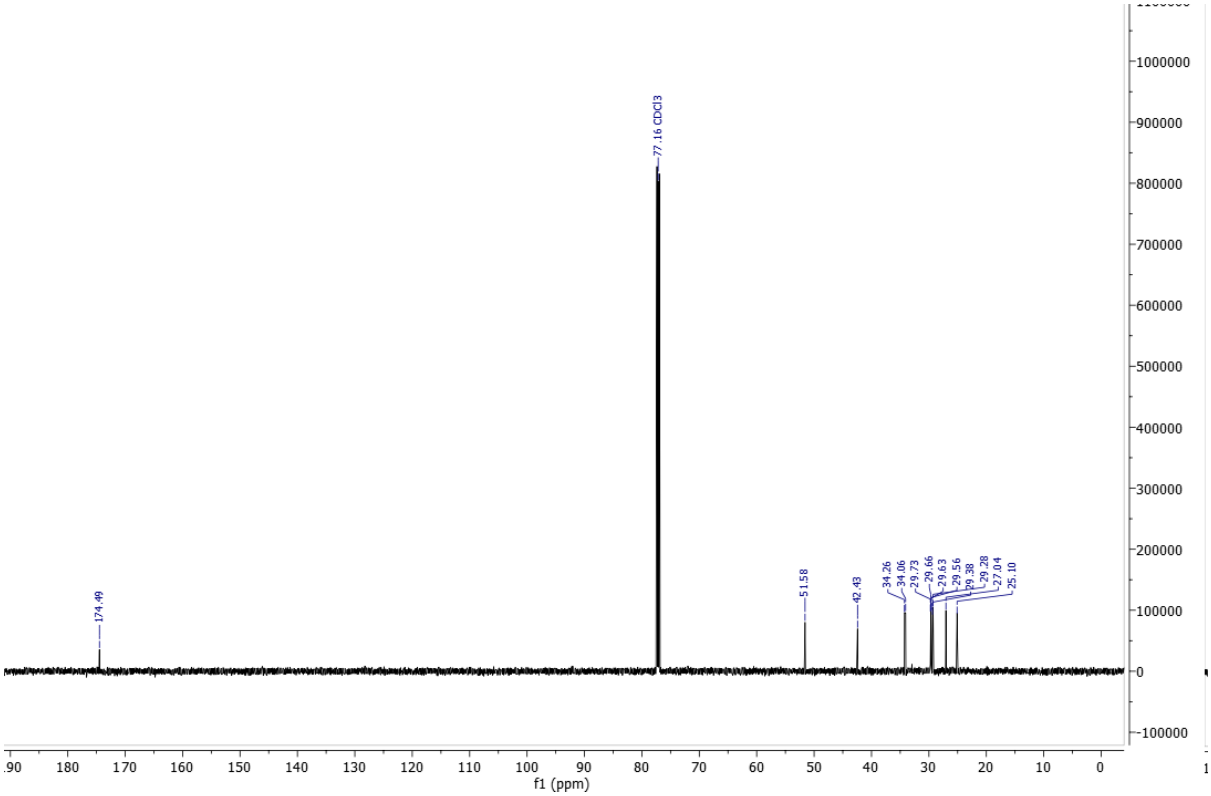

Figure S 26: ^{13}C NMR spectrum (151 MHz) methyl-12-aminododecanoate (**3f**) in $CDCl_3$.

Benzaldehyde oxime (1g)

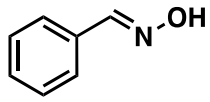

^{1}H NMR (600 MHz, $CDCl_3$) δ = 8.18 (t, *J* = 1.5 Hz, 1H), 7.59 (dd, *J* = 6.7, 3.0 Hz, 2H), 7.42 – 7.37 (m, 3H).

^{13}C NMR (151 MHz, $CDCl_3$) δ = 150.47, 132.02, 131.11, 130.37, 130.24, 128.94, 128.65, 128.59, 127.19.

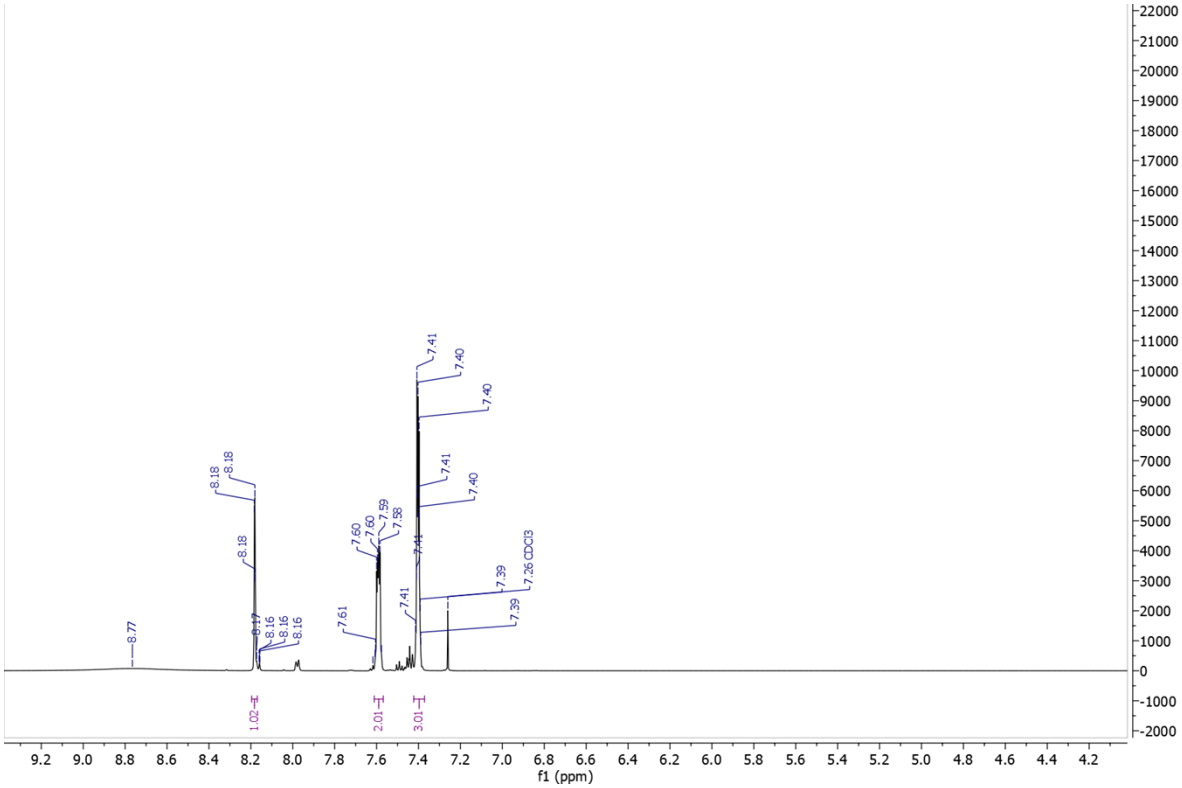

Figure S 27: ^{1}H NMR spectrum (600 MHz) of benzaldehyde oxime (**1g**) in $CDCl_3$.

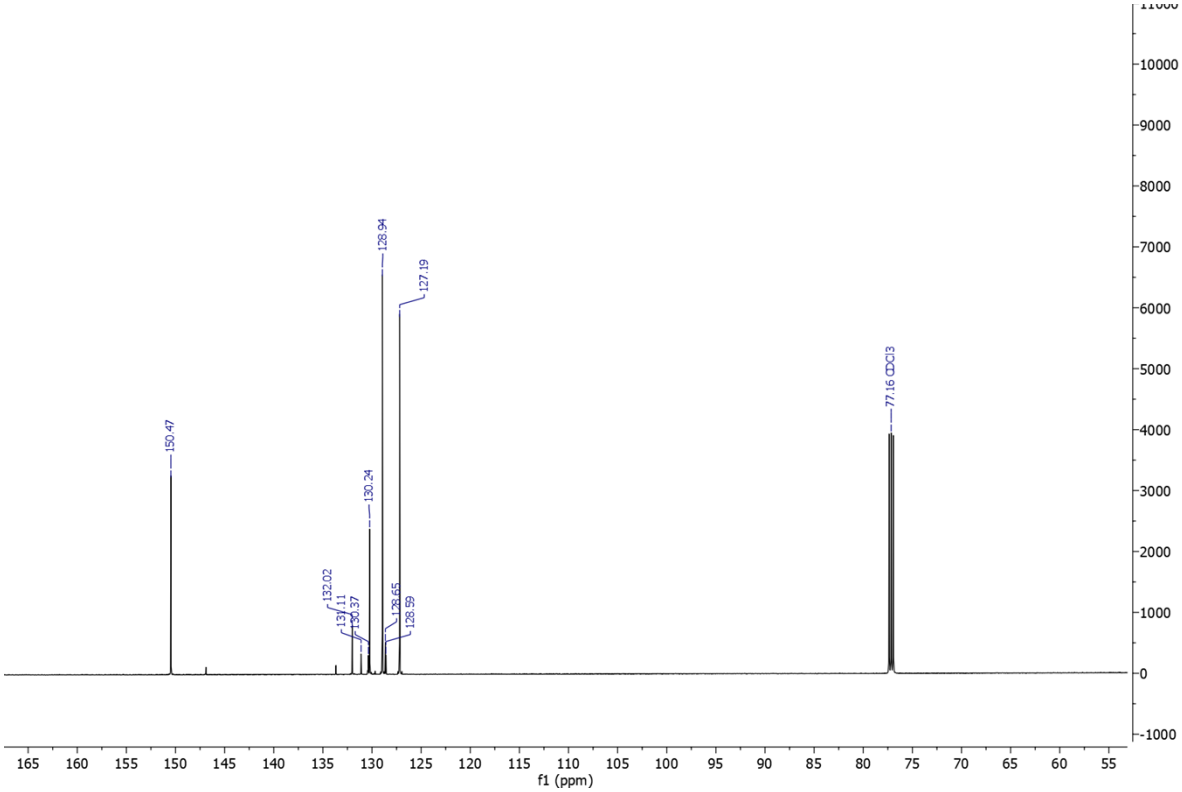

Figure S 28: ^{13}C NMR spectrum (151 MHz) of benzaldehyde oxime (**1g**) in $CDCl_3$.

(6-bromopyridin-2-yl)methanamine (3h)

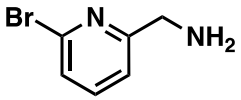

^{1}H NMR (600 MHz, CDCl3) δ = 7.50 (t, *J* = 7.7 Hz, 1H), 7.34 (dd, *J* = 7.8, 0.9 Hz, 1H), 7.27 – 7.24 (m, 1H), 3.94 (s, 2H), 1.72 (s, 2H).

^{13}C NMR (151 MHz, CDCl3) δ = 163.99, 141.95, 139.07, 126.28, 120.08, 47.54.

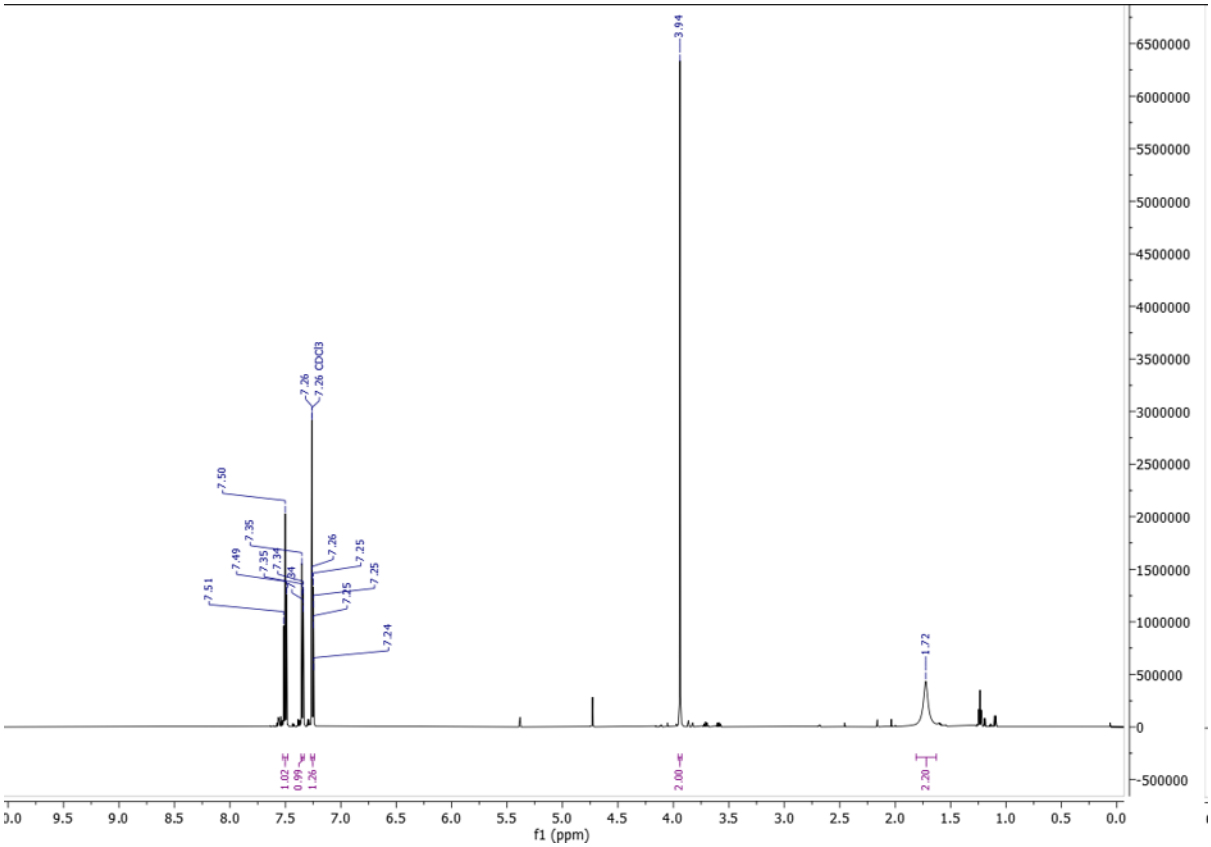

Figure S 29: ^{1}H NMR spectrum (600 MHz) of (6-bromopyridin-2-yl)methanamine (**3h**) in $CDCl_3$.

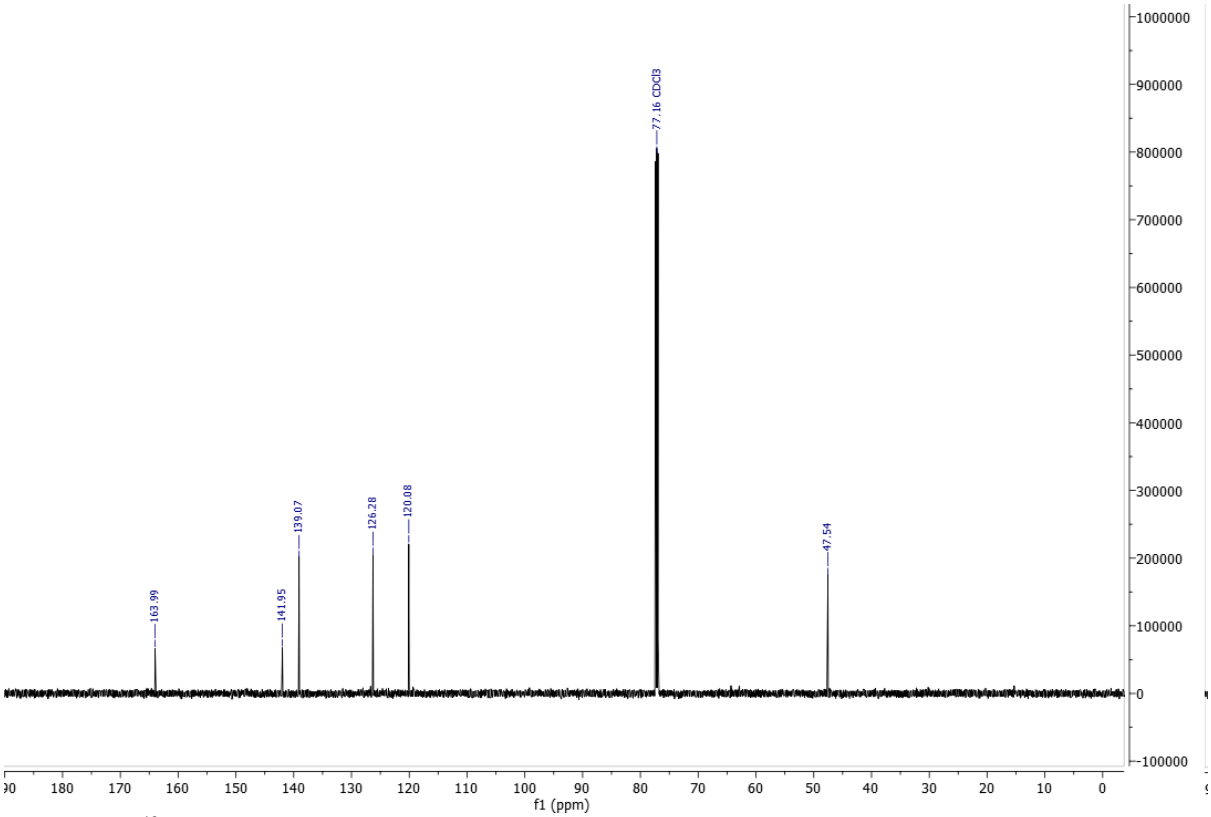

Figure S 30: ^{13}C NMR spectrum (151 MHz) of (6-bromopyridin-2-yl)methanamine (**3h**) in $CDCl_3$.

Furfuryl oxime (1i):

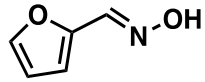

^{1}H NMR (400 MHz, $CDCl_3$) δ = 10.01 (s, 5H), 8.03 (s, 1H), 7.54 (s, 4H), 7.50 (dd, *J* = 1.7, 0.7 Hz, 2H), 7.48 (dd, *J* =1.7, 0.7 Hz, 5H), 7.35 (dd, *J* =3.4, 1.0 Hz, 5H), 6.65 (d, *J* = 3.4 Hz, 2H), 6.54 (ddd, *J* = 3.5, 1.8, 0.7 Hz, 6H), 6.46 (dd, *J* = 3.5, 1.8 Hz, 2H).

^{13}C NMR (101 MHz, $CDCl_3$) δ = 147.22, 145.23, 144.45, 143.59, 140.32, 137.21, 118.38, 112.87, 112.44, 111.72.

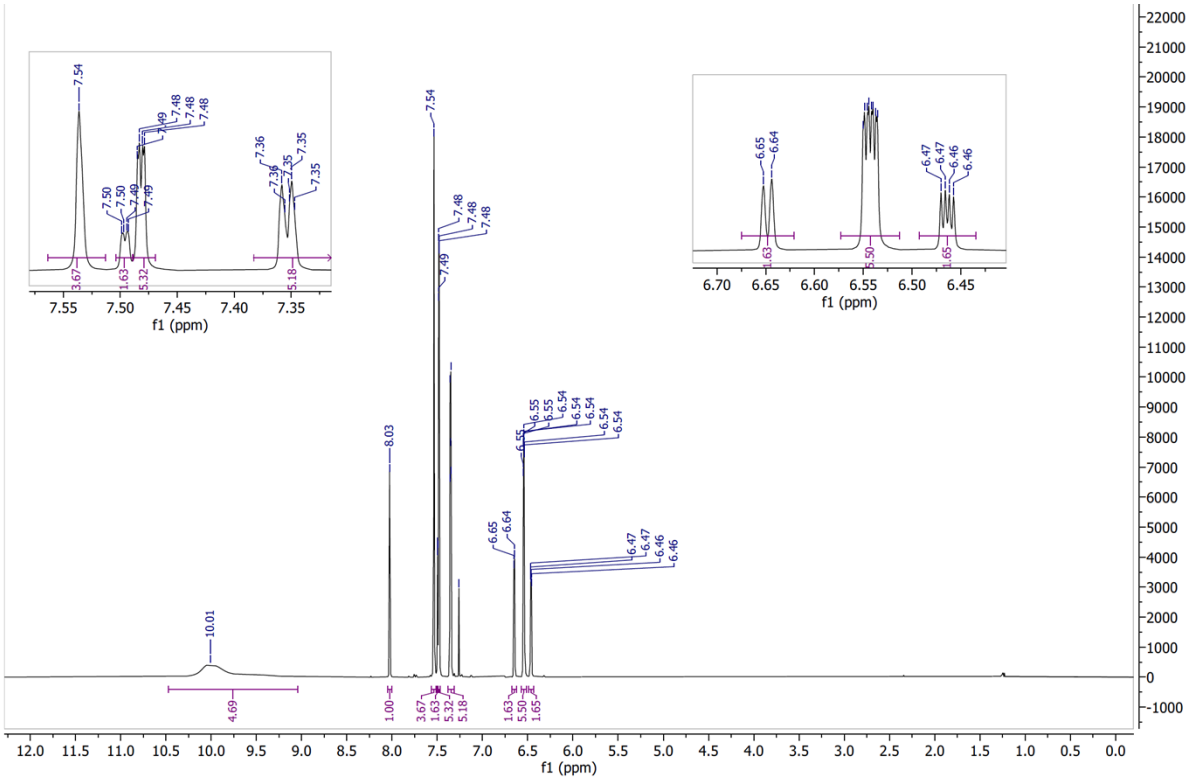

Figure S 31: ^{1}H NMR spectrum (400 MHz) of furfuryl oxime (**1i**) in $CDCl_3$.

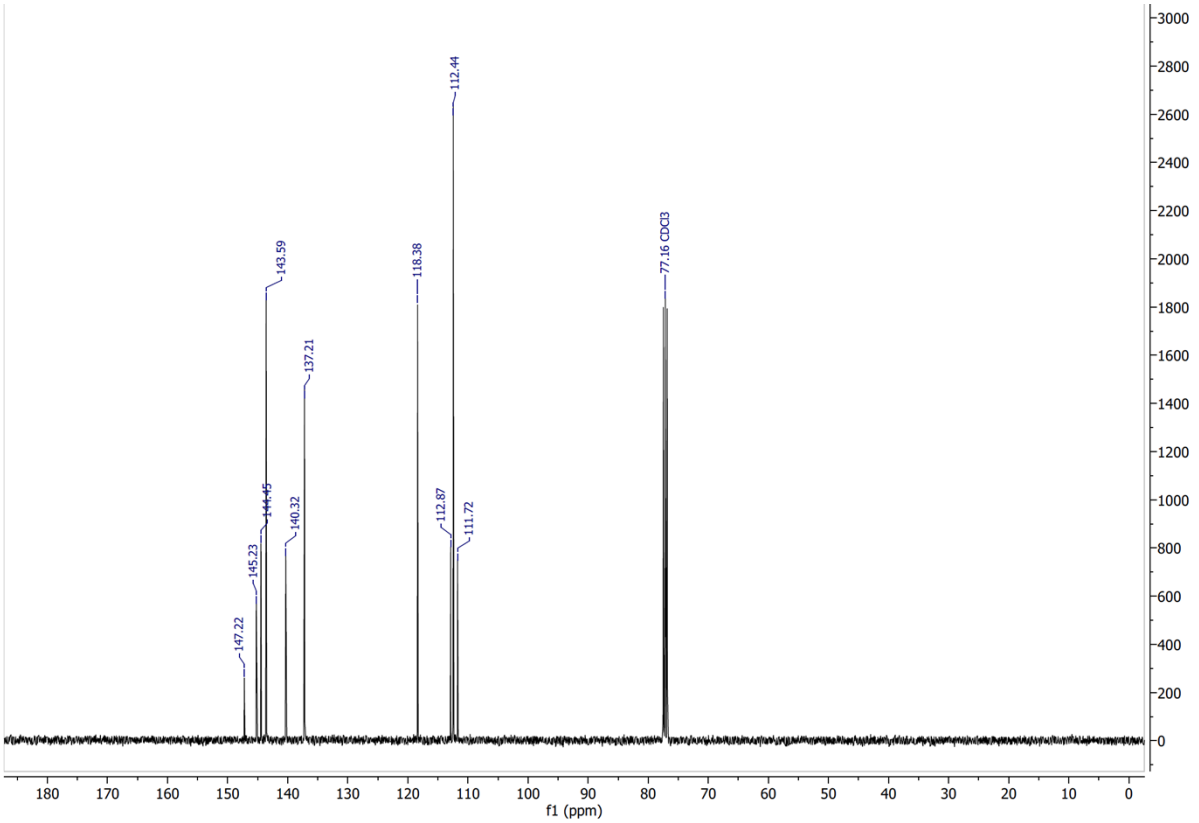

Figure S 32: ^{13}C NMR spectrum (101 MHz) of furfuryl oxime (**1i**) in $CDCl_3$.

GC Analysis

All chromatograms were recorded by an AGILENT 7890A gas chromatograph with an HP-5-column (length = 30 m, diameter = 0.25 mm, film thickness = 25 µm). Each sample was measured with a split ratio of 75:1 and a sample volume of 1 µL. The species were determined by previous calibrations (Figure S 33). The corresponding heating profile for the hydrogenation of hexanal oxime (**1a**) is shown in Table S 2. The heating profiles for the substrate screening are shown subsequently).

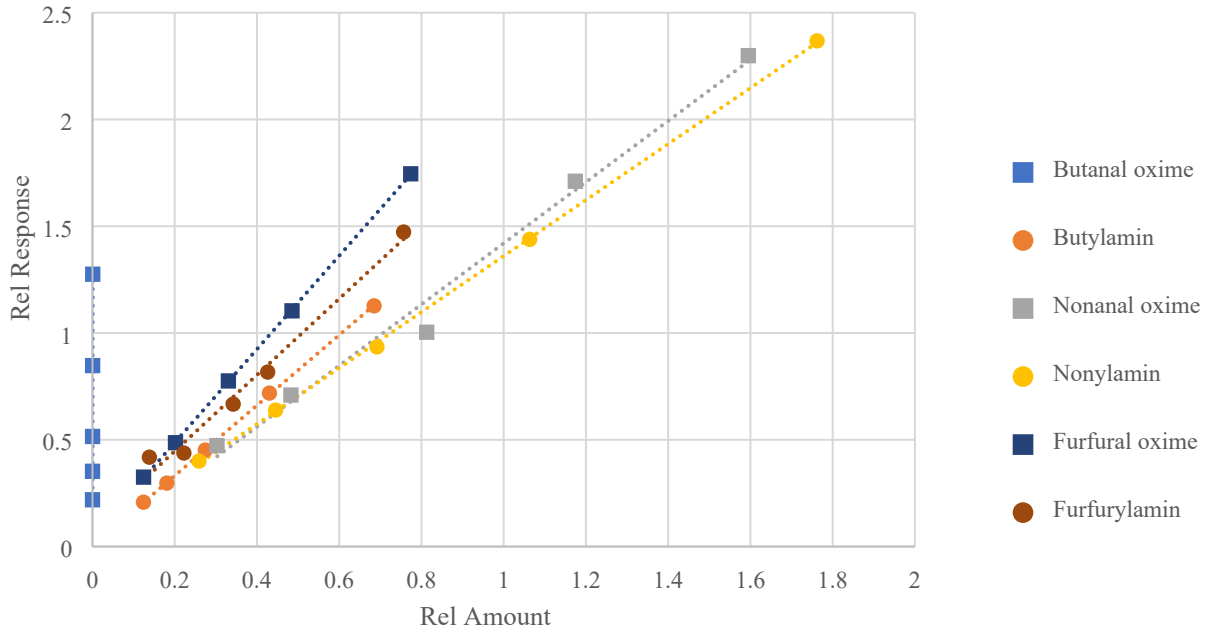

Figure S 33: Calibration curve for GC Analysis.

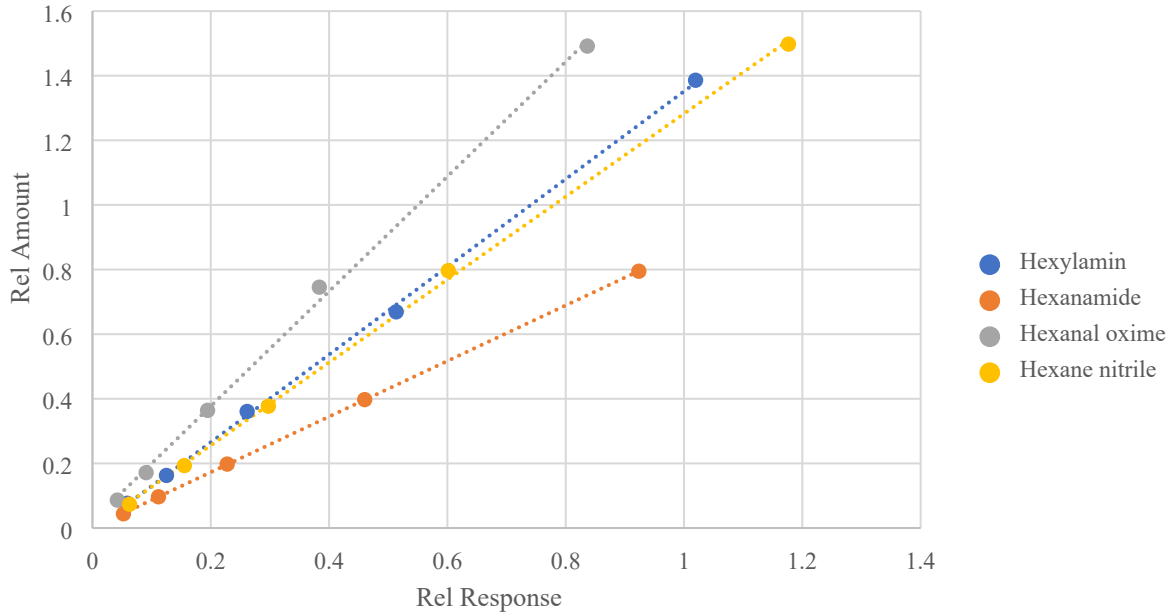

Figure S 34: Calibration curve for C_6 substrates and intermediates.

Table S 2: Temperature profile of GC measurements with the method.

	Rate / °C min^{-1}	Value / °C	Hold Time / min	Run Time / min
Initial	0	60	0.5	0.5
Ramp 1	10	100	0	4.5
Ramp 2	15	110	0	5.17
Ramp 3	50	120	0	5.37
Ramp 4	15	130	0	6.0
Ramp 5	50	165	0	6.7
Ramp 6	18	275	0	12.8

Table S 3: Temperature profile for longer chained aliphatic oximes (~C_9)

	Rate / °C min^{-1}	Value / °C	Hold Time / min	Run Time / min
Initial	0	60	0.5	0.5
Ramp 1	50	120	0	1.7
Ramp 2	10	140	0	3.7
Ramp 3	5	150	1	6.7
Ramp 4	5	160	0	8.7
Ramp 5	15	200	0	11.37
Ramp 6	18	275	0	15.5

Table S 4: Temperature profile for long chains aliphatic oximes (C_{12}).

	Rate / °C min^{-1}	Value / °C	Hold Time / min	Run Time / min
Initial	0	60	0.5	0.5
Ramp 1	50	165	0	2.6
Ramp 2	20	275	3	11.1

HPLC-HRMS Spectra

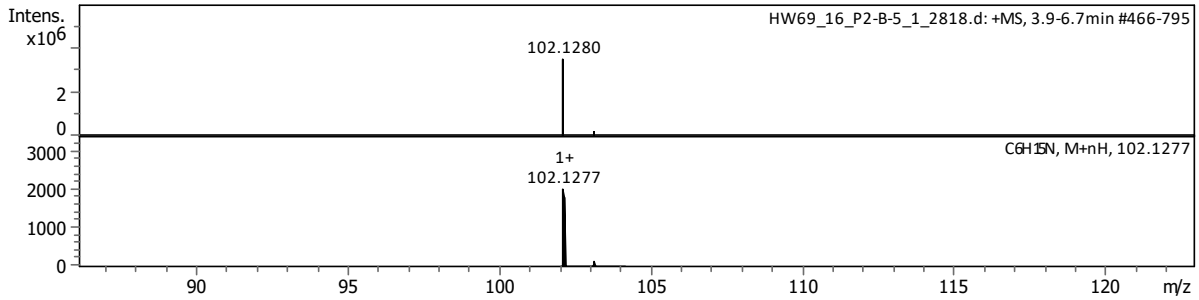

Figure S 35: LC-HRMS Spectra for hexylamine (**3a**) from the hydrogenation of hexanal oxime (**1a**), top measured, bottom calculated.

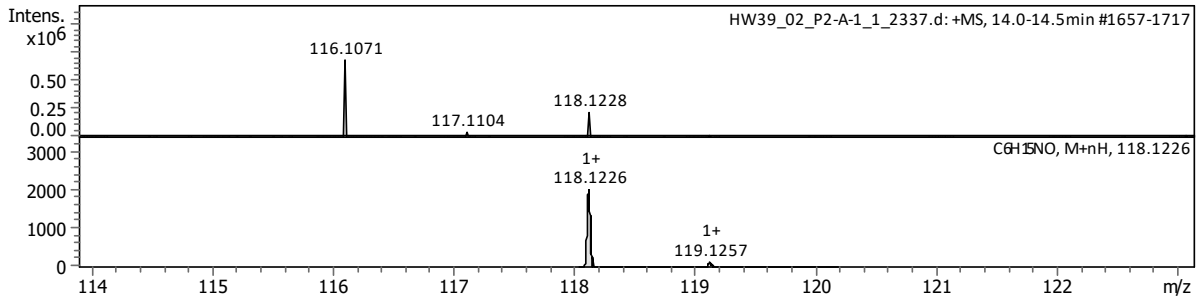

Figure S 36: LC-HRMS Spectra for hexyl hydroxylamine (**2a**) from the hydrogenation of hexanal oxime (**1a**), top measured, bottom calculated.

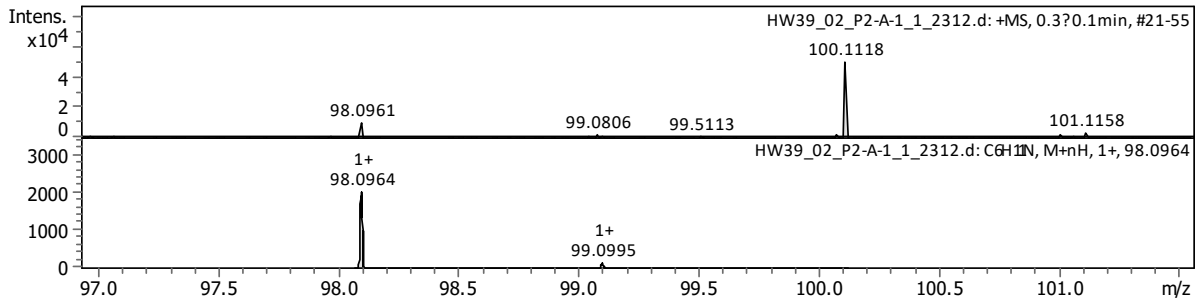

Figure S 37: LC-HRMS Spectra for hexanenitrile (**5a**) from the hydrogenation of hexanal oxime (**1a**), top measured, bottom calculated.

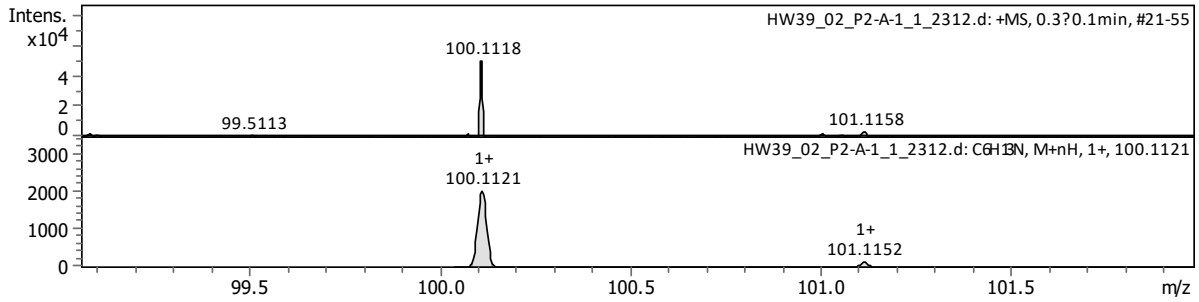

Figure S 38: LC-HRMS Spectra for hexylimine (**6a**) from the hydrogenation of hexanal oxime (**1a**), top measured, bottom calculated.

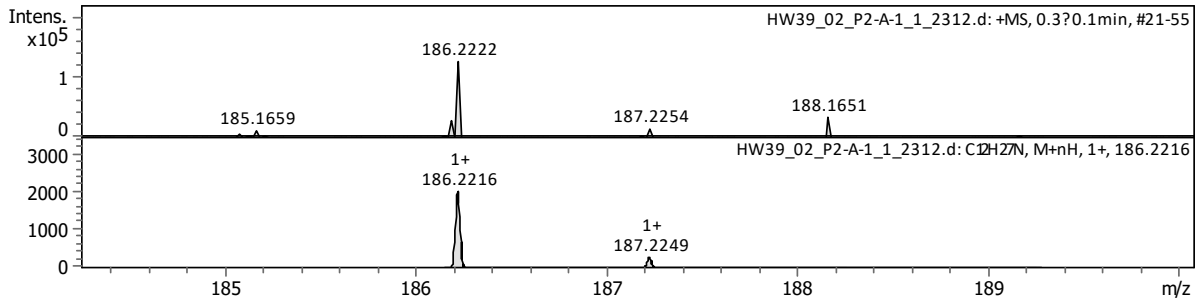

Figure S 39: LC-HRMS Spectra for dihexylamine (**7a**) from the hydrogenation of hexanal oxime (**1a**), top measured, bottom calculated.

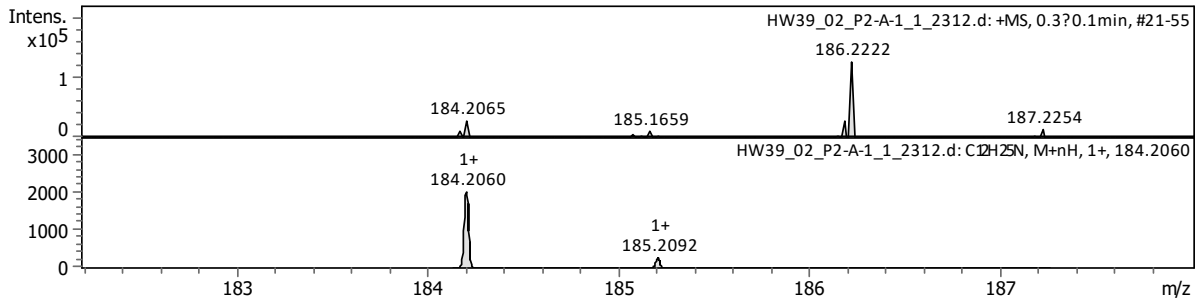

Figure S 40: LC-HRMS Spectra for dihexylimine from the hydrogenation of hexanal oxime (**1a**), top measured, bottom calculated.

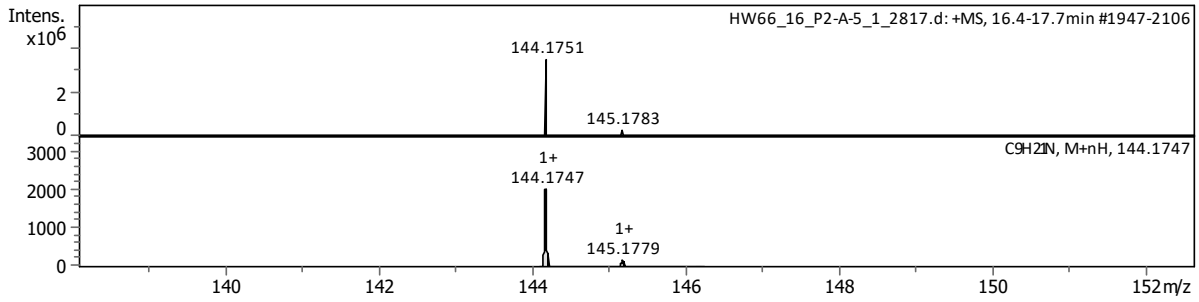

Figure S 41: LC-HRMS Spectra for nonylamine from the hydrogenation of nonanal oxime, top measured, bottom calculated.